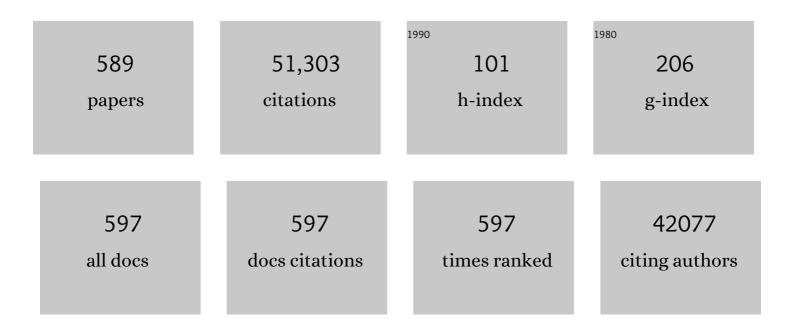
List of Publications by Year in descending order

Source: https://exaly.com/author-pdf/507106/publications.pdf Version: 2024-02-01



| #  | Article  | lF   | CITATIONS |
|----|--|------|-----------|
| 1  | Epitaxial BiFeO3 Multiferroic Thin Film Heterostructures. Science, 2003, 299, 1719-1722.   | 6.0  | 5,548     |
| 2  | Pseudocapacitive Contributions to Electrochemical Energy Storage in TiO <sub>2</sub> (Anatase)<br>Nanoparticles. Journal of Physical Chemistry C, 2007, 111, 14925-14931.                            | 1.5  | 3,863     |
| 3  | Ordered mesoporous α-MoO3 with iso-oriented nanocrystalline walls for thin-film pseudocapacitors.<br>Nature Materials, 2010, 9, 146-151.   | 13.3 | 2,801     |
| 4  | Multiferroic BaTiO3-CoFe2O4 Nanostructures. Science, 2004, 303, 661-663.   | 6.0  | 2,051     |
| 5  | Rational Design of Metalâ€Organic Framework Derived Hollow NiCo <sub>2</sub> O <sub>4</sub> Arrays<br>for Flexible Supercapacitor and Electrocatalysis. Advanced Energy Materials, 2017, 7, 1602391. | 10.2 | 874       |
| 6  | Two dimensional hexagonal boron nitride (2D-hBN): synthesis, properties and applications. Journal of<br>Materials Chemistry C, 2017, 5, 11992-12022.   | 2.7  | 732       |
| 7  | Graphene-based materials for supercapacitor electrodes – A review. Journal of Materiomics, 2016, 2,<br>37-54.  | 2.8  | 620       |
| 8  | Hollow Mo-doped CoP nanoarrays for efficient overall water splitting. Nano Energy, 2018, 48, 73-80.  | 8.2  | 608       |
| 9  | A Highâ€Rate and Stable Quasiâ€Solidâ€State Zincâ€Ion Battery with Novel 2D Layered Zinc Orthovanadate<br>Array. Advanced Materials, 2018, 30, e1803181.   | 11.1 | 571       |
| 10 | Intrinsically fluorescent carbon dots with tunable emission derived from hydrothermal treatment of glucose in the presence of monopotassium phosphate. Chemical Communications, 2011, 47, 11615.     | 2.2  | 529       |
| 11 | Hafnia and hafnia-toughened ceramics. Journal of Materials Science, 1992, 27, 5397-5430.   | 1.7  | 511       |
| 12 | A Flexible Quasiâ€Solidâ€State Nickel–Zinc Battery with High Energy and Power Densities Based on 3D<br>Electrode Design. Advanced Materials, 2016, 28, 8732-8739.                                    | 11.1 | 479       |
| 13 | Multiferroic bismuth ferrite-based materials for multifunctional applications: Ceramic bulks, thin films and nanostructures. Progress in Materials Science, 2016, 84, 335-402.                       | 16.0 | 478       |
| 14 | Iron Oxide-Decorated Carbon for Supercapacitor Anodes with Ultrahigh Energy Density and Outstanding Cycling Stability. ACS Nano, 2015, 9, 5198-5207.   | 7.3  | 441       |
| 15 | Hollow Co <sub>3</sub> O <sub>4</sub> Nanosphere Embedded in Carbon Arrays for Stable and Flexible Solid tate Zinc–Air Batteries. Advanced Materials, 2017, 29, 1704117.                             | 11.1 | 407       |
| 16 | In Situ Grown Epitaxial Heterojunction Exhibits Highâ€Performance Electrocatalytic Water Splitting.<br>Advanced Materials, 2018, 30, e1705516.   | 11.1 | 375       |
| 17 | Zirconia-toughened alumina (ZTA) ceramics. Journal of Materials Science, 1989, 24, 3421-3440.  | 1.7  | 372       |
| 18 | Single Co Atoms Anchored in Porous N-Doped Carbon for Efficient Zincâ^'Air Battery Cathodes. ACS<br>Catalysis, 2018, 8, 8961-8969.   | 5.5  | 364       |

| #  | Article  | IF  | CITATIONS |
|----|--|---|-----------|
| 19 | Metal Phosphides and Phosphatesâ€based Electrodes for Electrochemical Supercapacitors. Small, 2017, 13, 1701530.   | 5.2   | 318       |
| 20 | Ferroelectricity of CH <sub>3</sub> NH <sub>3</sub> PbI <sub>3</sub> Perovskite. Journal of Physical Chemistry Letters, 2015, 6, 1155-1161.  | 2.1   | 295       |
| 21 | Copper Single Atoms Anchored in Porous Nitrogen-Doped Carbon as Efficient pH-Universal Catalysts for the Nitrogen Reduction Reaction. ACS Catalysis, 2019, 9, 10166-10173.   | 5.5   | 284       |
| 22 | Cactusâ€Like NiCoP/NiCoâ€OH 3D Architecture with Tunable Composition for Highâ€Performance<br>Electrochemical Capacitors. Advanced Functional Materials, 2018, 28, 1800036.  | 7.8   | 274       |
| 23 | Sulfur-doped cobalt phosphide nanotube arrays for highly stable hybrid supercapacitor. Nano Energy, 2017, 39, 162-171.   | 8.2   | 273       |
| 24 | Highâ€Performance Flexible Solidâ€State Ni/Fe Battery Consisting of Metal Oxides Coated Carbon<br>Cloth/Carbon Nanofiber Electrodes. Advanced Energy Materials, 2016, 6, 1601034.  | 10.2  | 262       |
| 25 | The growth of nickel-manganese and cobalt-manganese layered double hydroxides on reduced graphene oxide for supercapacitor. Electrochimica Acta, 2016, 206, 108-115.   | 2.6   | 259       |
| 26 | Effects of grain size on the dielectric properties and tunabilities of sol–gel derived Ba(Zr0.2Ti0.8)O3<br>ceramics. Solid State Communications, 2004, 131, 163-168.   | 0.9   | 252       |
| 27 | Epitaxial BiFeO3 thin films on Si. Applied Physics Letters, 2004, 85, 2574-2576.   | 1.5   | 249       |
| 28 | Metal–organic framework derived hollow CoS <sub>2</sub> nanotube arrays: an efficient<br>bifunctional electrocatalyst for overall water splitting. Nanoscale Horizons, 2017, 2, 342-348.   | 4.1   | 247       |
| 29 | Decorating Co/CoNx nanoparticles in nitrogen-doped carbon nanoarrays for flexible and rechargeable zinc-air batteries. Energy Storage Materials, 2019, 16, 243-250.  | 9.5   | 244       |
| 30 | MOF-derived nanohybrids for electrocatalysis and energy storage: current status and perspectives.<br>Chemical Communications, 2018, 54, 5268-5288.   | 2.2   | 237       |
| 31 | Perovskites for photovoltaics: a combined review of organic–inorganic halide perovskites and<br>ferroelectric oxide perovskites. Journal of Materials Chemistry A, 2015, 3, 18809-18828.   | 5.2   | 232       |
| 32 | TMD-based highly efficient electrocatalysts developed by combined computational and experimental approaches. Chemical Society Reviews, 2018, 47, 4332-4356.  | 18.7  | 232       |
| 33 | Oxygen-vacancy-related relaxation and scaling behaviors of <mml:math<br>xmlns:mml="http://www.w3.org/1998/Math/MathML"<br/>display="inline"&gt;<mml:mrow><mml:msub><mml:mrow><mml:mtext>Bi</mml:mtext></mml:mrow><mml:mrow><br/>Physical Review B. 2010. 82</mml:mrow></mml:msub></mml:mrow></mml:math<br> | < <b>1.1</b><br><mml:mn:< td=""><td>&gt;0.9</td></mml:mn:<> | >0.9      |
| 34 | Significant Role of Al in Ternary Layered Double Hydroxides for Enhancing Electrochemical<br>Performance of Flexible Asymmetric Supercapacitor. Advanced Functional Materials, 2019, 29, 1903879.  | 7.8   | 228       |
| 35 | Cobalt oxide and N-doped carbon nanosheets derived from a single two-dimensional metal–organic<br>framework precursor and their application in flexible asymmetric supercapacitors. Nanoscale<br>Horizons, 2017, 2, 99-105.  | 4.1   | 227       |
| 36 | Mechanochemical synthesis of nanocrystalline hydroxyapatite from CaO and CaHPO4. Biomaterials, 2001, 22, 2705-2712.  | 5.7   | 217       |

| #  | Article  | IF   | CITATIONS |
|----|--|------|-----------|
| 37 | Oneâ€dimensional and twoâ€dimensional synergized nanostructures for highâ€performing energy storage<br>and conversion. InformaÄnÃ-Materiály, 2020, 2, 3-32.  | 8.5  | 206       |
| 38 | Silica-based nanocapsules: synthesis, structure control and biomedical applications. Chemical Society Reviews, 2015, 44, 315-335.  | 18.7 | 205       |
| 39 | Rational Design of Holey 2D Nonlayered Transition Metal Carbide/Nitride Heterostructure Nanosheets<br>for Highly Efficient Water Oxidation. Advanced Energy Materials, 2019, 9, 1803768.   | 10.2 | 204       |
| 40 | Surfaceâ€Chargeâ€Mediated Formation of Hâ€īiO <sub>2</sub> @Ni(OH) <sub>2</sub> Heterostructures for<br>Highâ€Performance Supercapacitors. Advanced Materials, 2017, 29, 1604164.  | 11.1 | 203       |
| 41 | (Ni,Co)Se <sub>2</sub> /NiCoâ€LDH Core/Shell Structural Electrode with the Cactusâ€Like<br>(Ni,Co)Se <sub>2</sub> Core for Asymmetric Supercapacitors. Small, 2019, 15, e1803895.  | 5.2  | 203       |
| 42 | Hierarchical Microâ€Nano Sheet Arrays of Nickel–Cobalt Double Hydroxides for Highâ€Rate Ni–Zn<br>Batteries. Advanced Science, 2019, 6, 1802002.  | 5.6  | 202       |
| 43 | CuO nanowires synthesized by thermal oxidation route. Journal of Alloys and Compounds, 2008, 454, 268-273.   | 2.8  | 200       |
| 44 | Controllable MnCo <sub>2</sub> S <sub>4</sub> nanostructures for high performance hybrid supercapacitors. Journal of Materials Chemistry A, 2017, 5, 7494-7506.  | 5.2  | 198       |
| 45 | Efficient Hydrogen Evolution of Oxidized Niâ€N <sub>3</sub> Defective Sites for Alkaline Freshwater<br>and Seawater Electrolysis. Advanced Materials, 2021, 33, e2003846.  | 11.1 | 198       |
| 46 | Composition and poling condition-induced electrical behavior of (Ba0.85Ca0.15)(Ti1â^'xZrx)O3 lead-free piezoelectric ceramics. Journal of the European Ceramic Society, 2012, 32, 891-898.   | 2.8  | 197       |
| 47 | 3Dâ€Printed MOFâ€Derived Hierarchically Porous Frameworks for Practical Highâ€Energy Density<br>Li–O <sub>2</sub> Batteries. Advanced Functional Materials, 2019, 29, 1806658.   | 7.8  | 197       |
| 48 | All‣olid‣tate Fiber Supercapacitors with Ultrahigh Volumetric Energy Density and Outstanding<br>Flexibility. Advanced Energy Materials, 2019, 9, 1802753.  | 10.2 | 197       |
| 49 | Synthesis of Fe3O4 nanoparticles from emulsions. Journal of Materials Chemistry, 2001, 11, 1704-1709.  | 6.7  | 193       |
| 50 | Integrated Hierarchical Carbon Flake Arrays with Hollow Pâ€Đoped CoSe <sub>2</sub> Nanoclusters as<br>an Advanced Bifunctional Catalyst for Zn–Air Batteries. Advanced Functional Materials, 2018, 28,<br>1804846.                               | 7.8  | 192       |
| 51 | Synergizing Mo Single Atoms and Mo <sub>2</sub> C Nanoparticles on CNTs Synchronizes Selectivity<br>and Activity of Electrocatalytic N <sub>2</sub> Reduction to Ammonia. Advanced Materials, 2020, 32,<br>e2002177.                             | 11.1 | 190       |
| 52 | Stitching of Zn <sub>3</sub> (OH) <sub>2</sub> V <sub>2</sub> O <sub>7</sub> ·2H <sub>2</sub> O 2D<br>Nanosheets by 1D Carbon Nanotubes Boosts Ultrahigh Rate for Wearable Quasi-Solid-State Zinc-Ion<br>Batteries. ACS Nano, 2020, 14, 842-853. | 7.3  | 183       |
| 53 | Ni-Doped Cobalt–Cobalt Nitride Heterostructure Arrays for High-Power Supercapacitors. ACS Energy<br>Letters, 2018, 3, 2462-2469.   | 8.8  | 182       |
| 54 | Ceramic-based membranes for water and wastewater treatment. Colloids and Surfaces A:<br>Physicochemical and Engineering Aspects, 2019, 578, 123513.  | 2.3  | 179       |

| #  | Article  | IF        | CITATIONS |
|----|--|-----------|-----------|
| 55 | Bimetallic Nickel Cobalt Sulfide as Efficient Electrocatalyst for Zn–Air Battery and Water Splitting.<br>Nano-Micro Letters, 2019, 11, 2.  | 14.4      | 179       |
| 56 | Generation and Dynamics of an Endogenous, Self-Generated Signaling Gradient across a Migrating Tissue. Cell, 2013, 155, 674-687.   | 13.5      | 174       |
| 57 | Potential-Dependent Phase Transition and Mo-Enriched Surface Reconstruction of γ-CoOOH in a<br>Heterostructured Co-Mo <sub>2</sub> C Precatalyst Enable Water Oxidation. ACS Catalysis, 2020, 10,<br>4411-4419.                        | 5.5       | 174       |
| 58 | Improving the magnetic properties of hydrothermally synthesized barium ferrite. Journal of<br>Magnetism and Magnetic Materials, 1999, 195, 452-459.  | 1.0       | 172       |
| 59 | NiFe2O4 ultrafine particles prepared by co-precipitation/mechanical alloying. Journal of Magnetism and Magnetic Materials, 1999, 205, 249-254.   | 1.0       | 170       |
| 60 | Role of room-temperature phase transition in the electrical properties of (Ba, Ca)(Ti, Zr)O3 ceramics.<br>Scripta Materialia, 2011, 65, 771-774.   | 2.6       | 170       |
| 61 | NiFe2O4 nanoparticles formed in situ in silica matrix by mechanical activation. Journal of Applied Physics, 2002, 91, 6015-6020.   | 1.1       | 165       |
| 62 | Fabrication of (NH4)2V3O8 nanoparticles encapsulated in amorphous carbon for high capacity electrodes in aqueous zinc ion batteries. Chemical Engineering Journal, 2020, 382, 122844.  | 6.6       | 164       |
| 63 | Ferroelectric HfO <sub>2</sub> -based materials for next-generation ferroelectric memories. Journal of Advanced Dielectrics, 2016, 06, 1630003.  | 1.5       | 163       |
| 64 | Manipulating unidirectional fluid transportation to drive sustainable solar water extraction and brine-drenching induced energy generation. Energy and Environmental Science, 2020, 13, 4891-4902.                                     | 15.6      | 162       |
| 65 | Heterojunction engineering of MoSe2/MoS2 with electronic modulation towards synergetic<br>hydrogen evolution reaction and supercapacitance performance. Chemical Engineering Journal, 2019,<br>359, 1419-1426.                         | 6.6       | 160       |
| 66 | Intrinsically fluorescent nitrogen-containing carbon nanoparticles synthesized by a hydrothermal process. Carbon, 2011, 49, 5207-5212.   | 5.4       | 156       |
| 67 | Selfâ€Powered Waterâ€5plitting Devices by Core–Shell NiFe@Nâ€Graphiteâ€Based Zn–Air Batteries. Advanc<br>Functional Materials, 2018, 28, 1706928.  | ed<br>7.8 | 155       |
| 68 | Mechanochemical Synthesis of Lead Zirconate Titanate from Mixed Oxides. Journal of the American<br>Ceramic Society, 1999, 82, 1687-1692.   | 1.9       | 154       |
| 69 | Nanoframes of Co <sub>3</sub> O <sub>4</sub> –Mo <sub>2</sub> N Heterointerfaces Enable<br>Highâ€Performance Bifunctionality toward Both Electrocatalytic HER and OER. Advanced Functional<br>Materials, 2022, 32, 2107382.            | 7.8       | 153       |
| 70 | Synthesis and piezoresponse of highly ordered Pb(Zr0.53Ti0.47)O3 nanowire arrays. Applied Physics<br>Letters, 2004, 85, 4190-4192.   | 1.5       | 151       |
| 71 | Processing of hydroxyapatite via microemulsion and emulsion routes. Biomaterials, 1997, 18, 1433-1439.   | 5.7       | 146       |
| 72 | Flexible Asymmetric Supercapacitor Based on Structureâ€Optimized<br>Mn <sub>3</sub> O <sub>4</sub> /Reduced Graphene Oxide Nanohybrid Paper with High Energy and<br>Power Density. Advanced Functional Materials, 2015, 25, 7291-7299. | 7.8       | 146       |

| #  | Article  | IF   | CITATIONS |
|----|--|------|-----------|
| 73 | An ultrafine barium ferrite powder of high coercivity from water-in-oil microemulsion. Journal of<br>Magnetism and Magnetic Materials, 1998, 184, 344-354.   | 1.0  | 145       |
| 74 | Transparent nanohybrids of nanocrystalline TiO2 in PMMA with unique nonlinear optical behavior.<br>Journal of Materials Chemistry, 2003, 13, 1475.   | 6.7  | 144       |
| 75 | Controlling the crystallinity and nonlinear optical properties of transparent TiO2–PMMA<br>nanohybrids. Journal of Materials Chemistry, 2004, 14, 2978-2987.   | 6.7  | 144       |
| 76 | Ferroelectric and Impedance Behavior of La―and Ti odoped BiFeO <sub>3</sub> Thin Films. Journal of the American Ceramic Society, 2010, 93, 2795-2803.  | 1.9  | 142       |
| 77 | BiFeO3 thin films of (1 1 1)-orientation deposited on SrRuO3 buffered Pt/TiO2/SiO2/Si(1 0 0) substrates.<br>Acta Materialia, 2010, 58, 1688-1697.  | 3.8  | 141       |
| 78 | Impedance study of giant dielectric permittivity in BaFe0.5Nb0.5O3 perovskite ceramic. Current Applied<br>Physics, 2010, 10, 21-25.  | 1.1  | 141       |
| 79 | Zn <sup>2+</sup> Preâ€Intercalation Stabilizes the Tunnel Structure of MnO <sub>2</sub> Nanowires<br>and Enables Zincâ€Ion Hybrid Supercapacitor of Batteryâ€Level Energy Density. Small, 2020, 16, e2000091.                            | 5.2  | 139       |
| 80 | Design and Manufacture of 3D-Printed Batteries. Joule, 2021, 5, 89-114.  | 11.7 | 137       |
| 81 | Synthesis of PEOlated Fe <sub>3</sub> O <sub>4</sub> @SiO <sub>2</sub> Nanoparticles via Bioinspired<br>Silification for Magnetic Resonance Imaging. Advanced Functional Materials, 2010, 20, 722-731.                                   | 7.8  | 132       |
| 82 | Electrocatalytic reduction of oxygen by a platinum nanoparticle/carbon nanotube composite electrode. Journal of Electroanalytical Chemistry, 2005, 577, 295-302.   | 1.9  | 130       |
| 83 | Effects of nitrogen doping on supercapacitor performance of a mesoporous carbon electrode<br>produced by a hydrothermal soft-templating process. Journal of Materials Chemistry A, 2014, 2, 11753.                                       | 5.2  | 127       |
| 84 | Ferroelectric and electrical behavior of (Na0.5Bi0.5)TiO3 thin films. Applied Physics Letters, 2004, 85, 804-806.  | 1.5  | 126       |
| 85 | Synergizing in-grown Ni3N/Ni heterostructured core and ultrathin Ni3N surface shell enables<br>self-adaptive surface reconfiguration and efficient oxygen evolution reaction. Nano Energy, 2020, 78,<br>105355.                          | 8.2  | 126       |
| 86 | Freestanding Metal–Organic Frameworks and Their Derivatives: An Emerging Platform for<br>Electrochemical Energy Storage and Conversion. Chemical Reviews, 2022, 122, 10087-10125.  | 23.0 | 126       |
| 87 | CuCo <sub>2</sub> S <sub>4</sub> Nanosheets@Nâ€Doped Carbon Nanofibers by Sulfurization at Room<br>Temperature as Bifunctional Electrocatalysts in Flexible Quasiâ€Solidâ€State Zn–Air Batteries. Advanced<br>Science, 2019, 6, 1900628. | 5.6  | 123       |
| 88 | Aqueous Rechargeable Multivalent Metalâ€ion Batteries: Advances and Challenges. Advanced Energy<br>Materials, 2021, 11, 2100608.   | 10.2 | 122       |
| 89 | Conformal dispersed cobalt nanoparticles in hollow carbon nanotube arrays for flexible Zn-air and<br>Al-air batteries. Chemical Engineering Journal, 2019, 369, 988-995.   | 6.6  | 121       |
| 90 | Porous NiCo2S4/FeOOH nanowire arrays with rich sulfide/hydroxide interfaces enable high OER<br>activity. Nano Energy, 2020, 78, 105230.  | 8.2  | 121       |

| #   | Article  | IF   | CITATIONS |
|-----|--|------|-----------|
| 91  | In situ coupled amorphous cobalt nitride with nitrogen-doped graphene aerogel as a trifunctional<br>electrocatalyst towards Zn-air battery deriven full water splitting. Applied Catalysis B:<br>Environmental, 2019, 259, 118100. | 10.8 | 120       |
| 92  | An improvement in processing of hydroxyapatite ceramics. Journal of Materials Science, 1995, 30, 3061-3074.  | 1.7  | 117       |
| 93  | 2D carbide nanomeshes and their assembling into 3D microflowers for efficient water splitting.<br>Applied Catalysis B: Environmental, 2019, 243, 678-685.  | 10.8 | 116       |
| 94  | Nurturing the marriages of single atoms with atomic clusters and nanoparticles for better heter heter heterogeneous electrocatalysis. , 2022, 1, 51-87.  |      | 114       |
| 95  | Heterogeneous Single Atom Electrocatalysis, Where "Singles―Are "Married― Advanced Energy<br>Materials, 2020, 10, 1903181.  | 10.2 | 113       |
| 96  | Gold-Cluster Sensors Formed Electrochemically at Boron-Doped-Diamond Electrodes: Detection of Dopamine in the Presence of Ascorbic Acid and Thiols. Advanced Functional Materials, 2005, 15, 639-647.                              | 7.8  | 110       |
| 97  | Activation of the MoSe <sub>2</sub> basal plane and Se-edge by B doping for enhanced hydrogen evolution. Journal of Materials Chemistry A, 2018, 6, 510-515.   | 5.2  | 110       |
| 98  | Ultrafast optical nonlinearity in poly(methylmethacrylate)-TiO2 nanocomposites. Applied Physics<br>Letters, 2003, 82, 2691-2693.   | 1.5  | 109       |
| 99  | Control of Synaptic Plasticity Learning of Ferroelectric Tunnel Memristor by Nanoscale Interface<br>Engineering. ACS Applied Materials & Interfaces, 2018, 10, 12862-12869.  | 4.0  | 109       |
| 100 | Effect of dwell time during sintering on piezoelectric properties of (Ba0.85Ca0.15)(Ti0.90Zr0.10)O3<br>lead-free ceramics. Journal of Alloys and Compounds, 2011, 509, L359-L361.  | 2.8  | 107       |
| 101 | Ferromagnetic, ferroelectric, and fatigue behavior of (111)-oriented BiFeO3/(Bi1/2Na1/2)TiO3 lead-free bilayered thin films. Applied Physics Letters, 2009, 94, .  | 1.5  | 106       |
| 102 | 3D-printed electrodes for lithium metal batteries with high areal capacity and high-rate capability.<br>Energy Storage Materials, 2020, 24, 336-342.   | 9.5  | 105       |
| 103 | Hollow Carbon Nanoparticles of Tunable Size and Wall Thickness by Hydrothermal Treatment of<br>α-Cyclodextrin Templated by F127 Block Copolymers. Chemistry of Materials, 2013, 25, 704-710.                                       | 3.2  | 103       |
| 104 | Conformally deposited NiO on a hierarchical carbon support for high-power and durable asymmetric supercapacitors. Journal of Materials Chemistry A, 2015, 3, 23283-23288.  | 5.2  | 103       |
| 105 | Bifunctional Oxygen Electrocatalyst of Mesoporous Ni/NiO Nanosheets for Flexible Rechargeable<br>Zn–Air Batteries. Nano-Micro Letters, 2020, 12, 68.   | 14.4 | 103       |
| 106 | Three Dimensionally Free-Formable Graphene Foam with Designed Structures for Energy and Environmental Applications. ACS Nano, 2020, 14, 937-947.   | 7.3  | 101       |
| 107 | All-in-one stretchable coaxial-fiber strain sensor integrated with high-performing supercapacitor.<br>Energy Storage Materials, 2020, 25, 124-130.   | 9.5  | 100       |
| 108 | Synthesizing Nanocrystalline Pb(Zn1/3Nb2/3)O3 Powders from Mixed Oxides. Journal of the American<br>Ceramic Society, 1999, 82, 477-479.  | 1.9  | 98        |

| #   | Article  | IF   | CITATIONS |
|-----|--|------|-----------|
| 109 | Formation of Nanocrystalline Hydroxyapatite in Nonionic Surfactant Emulsions. Langmuir, 1999, 15, 7472-7477.   | 1.6  | 97        |
| 110 | Processing of fine hydroxyapatite powders via an inverse microemulsion route. Materials Letters, 1996, 28, 431-436.  | 1.3  | 96        |
| 111 | Mutual Ferromagnetic–Ferroelectric Coupling in Multiferroic Copperâ€Doped ZnO. Advanced<br>Materials, 2011, 23, 1635-1640.   | 11.1 | 96        |
| 112 | Hybrid Fe <sub>2</sub> O <sub>3</sub> Nanoparticle Clusters/rGO Paper as an Effective Negative Electrode for Flexible Supercapacitors. Chemistry of Materials, 2016, 28, 7296-7303.                              | 3.2  | 95        |
| 113 | Surface nitridation of nickel-cobalt alloy nanocactoids raises the performance of water oxidation and splitting. Applied Catalysis B: Environmental, 2020, 270, 118889.  | 10.8 | 95        |
| 114 | Orientation dependence of ferroelectric behavior of BiFeO3 thin films. Journal of Applied Physics, 2009, 106, .  | 1.1  | 94        |
| 115 | Manganeseâ€Oxideâ€Based Electrode Materials for Energy Storage Applications: How Close Are We to the<br>Theoretical Capacitance?. Advanced Materials, 2018, 30, e1802569.  | 11.1 | 94        |
| 116 | Recent Progress in Twoâ€Dimensional Layered Double Hydroxides and Their Derivatives for<br>Supercapacitors. ChemSusChem, 2020, 13, 1226-1254.  | 3.6  | 94        |
| 117 | Engineering the Coordination Environment of Single Cobalt Atoms for Efficient Oxygen Reduction and Hydrogen Evolution Reactions. ACS Catalysis, 2021, 11, 4498-4509.   | 5.5  | 94        |
| 118 | Recent Development of Advanced Electrode Materials by Atomic Layer Deposition for Electrochemical Energy Storage. Advanced Science, 2016, 3, 1500405.  | 5.6  | 93        |
| 119 | Cage-confinement pyrolysis route to size-controlled molybdenum-based oxygen electrode catalysts:<br>From isolated atoms to clusters and nanoparticles. Nano Energy, 2020, 67, 104288.                            | 8.2  | 93        |
| 120 | Enhanced Photocatalysis by Doping Cerium into Mesoporous Titania Thin Films. Journal of Physical<br>Chemistry C, 2009, 113, 21406-21412.   | 1.5  | 92        |
| 121 | Ferroelectric Transistors with Nanowire Channel: Toward Nonvolatile Memory Applications. ACS<br>Nano, 2009, 3, 700-706.  | 7.3  | 89        |
| 122 | Electrical and magnetic properties of multiferroic BiFeO3/CoFe2O4 heterostructure. Journal of Applied Physics, 2008, 104, .  | 1.1  | 88        |
| 123 | Photovoltaic effect in an indium-tin-oxide/ZnO/BiFeO3/Pt heterostructure. Applied Physics Letters, 2014, 105, .  | 1.5  | 85        |
| 124 | Enlarged Interlayer Spacing in Cobalt–Manganese Layered Double Hydroxide Guiding Transformation<br>to Layered Structure for High Supercapacitance. ACS Applied Materials & Interfaces, 2019, 11,<br>23236-23243. | 4.0  | 85        |
| 125 | Z-scheme carbon-bridged Bi2O3/TiO2 nanotube arrays to boost photoelectrochemical detection performance. Applied Catalysis B: Environmental, 2019, 248, 255-263.  | 10.8 | 85        |
| 126 | Atomic layer deposition of Co <sub>3</sub> O <sub>4</sub> on carbon nanotubes/carbon cloth for high-capacitance and ultrastable supercapacitor electrode. Nanotechnology, 2015, 26, 094001.                      | 1.3  | 84        |

| #   | Article   | IF   | CITATIONS |
|-----|---|------|-----------|
| 127 | 3D Graphene-Nickel Hydroxide Hydrogel Electrode for High-Performance Supercapacitor.<br>Electrochimica Acta, 2016, 196, 653-660.  | 2.6  | 83        |
| 128 | Ultrafine Molybdenum Carbide Nanocrystals Confined in Carbon Foams via a Colloid onfinement<br>Route for Efficient Hydrogen Production. Small Methods, 2018, 2, 1700396.  | 4.6  | 83        |
| 129 | Mechanically Activating Nucleation and Growth of Complex Perovskites. Journal of Solid State Chemistry, 2000, 154, 321-328.   | 1.4  | 81        |
| 130 | Sintering temperature-induced electrical properties of (Ba0.90Ca0.10)(Ti0.85Zr0.15)O3 lead-free ceramics. Materials Research Bulletin, 2012, 47, 1281-1284.   | 2.7  | 81        |
| 131 | Direct observation of room-temperature out-of-plane ferroelectricity and tunneling electroresistance at the two-dimensional limit. Nature Communications, 2018, 9, 3319.  | 5.8  | 81        |
| 132 | NH <sub>4</sub> V <sub>3</sub> O <sub>8</sub> ·0.5H <sub>2</sub> O nanobelts with intercalated water<br>molecules as a high performance zinc ion battery cathode. Materials Chemistry Frontiers, 2020, 4,<br>1434-1443. | 3.2  | 81        |
| 133 | Effects of mechanical activation on the sintering and dielectric properties of oxide-derived PZT. Acta Materialia, 1999, 47, 2633-2639.   | 3.8  | 80        |
| 134 | Multiferroic behavior and impedance spectroscopy of bilayered BiFeO3/CoFe2O4 thin films. Journal of Applied Physics, 2009, 105, .   | 1.1  | 80        |
| 135 | 2D Metal–Organic Frameworks Derived Nanocarbon Arrays for Substrate Enhancement in Flexible<br>Supercapacitors. Small, 2018, 14, e1702641.  | 5.2  | 80        |
| 136 | 3D-Printing of Pure Metal–Organic Framework Monoliths. , 2019, 1, 147-153.  |      | 80        |
| 137 | Strain stabilized nickel hydroxide nanoribbons for efficient water splitting. Energy and Environmental Science, 2020, 13, 229-237.  | 15.6 | 78        |
| 138 | Binder-free 3D printing of covalent organic framework (COF) monoliths for CO2 adsorption.<br>Chemical Engineering Journal, 2021, 403, 126333.   | 6.6  | 78        |
| 139 | Size effect on the ferroelectric phase transition in SrBi2Ta2O9 nanoparticles. Journal of Applied Physics, 2003, 94, 618-620.   | 1.1  | 77        |
| 140 | 3D Nanostructure of Carbon Nanotubes Decorated Co 3 O 4 Nanowire Arrays for High Performance<br>Supercapacitor Electrode. Electrochimica Acta, 2015, 163, 9-15.   | 2.6  | 77        |
| 141 | Nanosized hydroxyapatite powders from microemulsions and emulsions stabilized by a biodegradable surfactant. Journal of Materials Chemistry, 1999, 9, 1635-1639.  | 6.7  | 75        |
| 142 | Metal–organic framework-derived integrated nanoarrays for overall water splitting. Journal of<br>Materials Chemistry A, 2018, 6, 9009-9018.   | 5.2  | 74        |
| 143 | Hollow spheres of nanocarbon and their manganese dioxide hybrids derived fromÂsoft template for supercapacitor application. Journal of Power Sources, 2013, 240, 713-720.   | 4.0  | 73        |
| 144 | Activation of sucrose-derived carbon spheres for high-performance supercapacitor electrodes. RSC Advances, 2015, 5, 9307-9313.  | 1.7  | 73        |

| #   | Article  | IF  | CITATIONS |
|-----|--|-----|-----------|
| 145 | Transition-metal-doped NiSe2 nanosheets towards efficient hydrogen evolution reactions. Nano<br>Research, 2018, 11, 6051-6061.   | 5.8 | 72        |
| 146 | Nanoflakes of Ni–Co LDH and Bi <sub>2</sub> O <sub>3</sub> Assembled in 3D Carbon Fiber Network<br>for High-Performance Aqueous Rechargeable Ni/Bi Battery. ACS Applied Materials & Interfaces,<br>2017, 9, 26008-26015. | 4.0 | 71        |
| 147 | Leakage mechanism of cation -modified BiFeO3 thin film. AIP Advances, 2011, 1, .   | 0.6 | 70        |
| 148 | Black Phosphorus@Ti <sub>3</sub> C <sub>2</sub> T <sub><i>x</i></sub> MXene Composites with<br>Engineered Chemical Bonds for Commercial-Level Capacitive Energy Storage. ACS Nano, 2021, 15,<br>12975-12987.             | 7.3 | 70        |
| 149 | Substrate-Assisted Crystallization and Photocatalytic Properties of Mesoporous TiO2 Thin Films.<br>Chemistry of Materials, 2006, 18, 2917-2923.  | 3.2 | 69        |
| 150 | Surfactant-modified chemically reduced graphene oxide for electrochemical supercapacitors. RSC Advances, 2014, 4, 26398-26406.   | 1.7 | 69        |
| 151 | Diblock Copolymer Templated Nanohybrid Thin Films of Highly Ordered TiO2Nanoparticle Arrays in PMMA Matrix. Chemistry of Materials, 2006, 18, 5876-5889.   | 3.2 | 68        |
| 152 | 3D TiO2@Ni(OH)2 Core-shell Arrays with Tunable Nanostructure for Hybrid Supercapacitor Application. Scientific Reports, 2015, 5, 13940.  | 1.6 | 68        |
| 153 | Ferroelectric domains and piezoelectricity in monocrystalline Pb(Zr,Ti)O3 nanowires. Applied Physics<br>Letters, 2007, 90, 133107.   | 1.5 | 67        |
| 154 | Flexible supercapacitor of high areal performance with vanadium/cobalt oxides on carbon nanofibers<br>as a binder-free membrane electrode. Chemical Engineering Journal, 2020, 402, 126294.                              | 6.6 | 67        |
| 155 | Unravelling V <sub>6</sub> O <sub>13</sub> Diffusion Pathways <i>via</i> CO <sub>2</sub><br>Modification for High-Performance Zinc Ion Battery Cathode. ACS Nano, 2021, 15, 1273-1281.                                   | 7.3 | 67        |
| 156 | Multiferroic BiFeO3 thin films deposited on SrRuO3 buffer layer by rf sputtering. Journal of Applied Physics, 2007, 101, 054104.   | 1.1 | 66        |
| 157 | Photoluminescence and Raman scattering studies on PbTiO3 nanowires fabricated by hydrothermal method at low temperature. Applied Physics Letters, 2006, 88, 193120.  | 1.5 | 65        |
| 158 | Effects of SrRuO3 buffer layer thickness on multiferroic (Bi0.90La0.10)(Fe0.95Mn0.05)O3 thin films.<br>Journal of Applied Physics, 2009, 106, .  | 1.1 | 65        |
| 159 | Stretchable fiber-shaped lithium metal anode. Energy Storage Materials, 2019, 22, 179-184.   | 9.5 | 65        |
| 160 | Ultrafine ferrite particles prepared by coprecipitation/mechanical milling. Materials Letters, 2000, 44, 19-22.  | 1.3 | 64        |
| 161 | Migration Kinetics of Oxygen Vacancies in Mn-Modified BiFeO <sub>3</sub> Thin Films. ACS Applied<br>Materials & Interfaces, 2011, 3, 2504-2511.  | 4.0 | 64        |
| 162 | Synthesis of monodispersed SnO2@C composite hollow spheres for lithium ion battery anode applications. Journal of Materials Chemistry, 2011, 21, 17448.  | 6.7 | 64        |

| #   | Article  | IF   | CITATIONS |
|-----|--|------|-----------|
| 163 | Lithiophilic polymer interphase anchored on laser-punched 3D holey Cu matrix enables uniform<br>lithium nucleation leading to super-stable lithium metal anodes. Energy Storage Materials, 2020, 29,<br>84-91. | 9.5  | 64        |
| 164 | PEOlated Micelle/Silica as Dual-Layer Protection of Quantum Dots for Stable and Targeted Bioimaging.<br>Chemistry of Materials, 2013, 25, 2976-2985.   | 3.2  | 63        |
| 165 | Key issues facing electrospun carbon nanofibers in energy applications: on-going approaches and challenges. Nanoscale, 2020, 12, 13225-13248.  | 2.8  | 63        |
| 166 | Giant strain in PbZr0.2Ti0.8O3 nanowires. Applied Physics Letters, 2007, 90, 052902.   | 1.5  | 62        |
| 167 | Design strategies for MOF-derived porous functional materials: Preserving surfaces and nurturing pores. Journal of Materiomics, 2021, 7, 440-459.  | 2.8  | 62        |
| 168 | Origin of a Tetragonal BiFeO <sub>3</sub> Phase with a Giant <i>c</i> / <i>a</i> Ratio on<br>SrTiO <sub>3</sub> Substrates. Advanced Functional Materials, 2012, 22, 937-942.                                  | 7.8  | 61        |
| 169 | Co/Zn bimetallic oxides derived from metal organic frameworks for high performance electrochemical energy storage. Electrochimica Acta, 2018, 291, 177-187.  | 2.6  | 60        |
| 170 | Wafer-scale solution-processed 2D material analog resistive memory array for memory-based computing. Nature Communications, 2022, 13, .  | 5.8  | 60        |
| 171 | Electrical behavior and oxygen vacancies in BiFeO3/[(Bi1/2Na1/2)0.94Ba0.06]TiO3 thin film. Applied Physics Letters, 2009, 95, .  | 1.5  | 59        |
| 172 | Co-sensitization of TiO2 by PbS quantum dots and dye N719 in dye-sensitized solar cells. Thin Solid<br>Films, 2010, 518, e54-e56.  | 0.8  | 59        |
| 173 | Intercalating graphene with clusters of Fe <sub>3</sub> O <sub>4</sub> nanocrystals for electrochemical supercapacitors. Materials Research Express, 2014, 1, 025015.  | 0.8  | 59        |
| 174 | Dynamic Surface Chemistry of Catalysts in Oxygen Evolution Reaction. Small Science, 2021, 1, 2100011.  | 5.8  | 59        |
| 175 | Top-seeding melt texture growth of single-domain superconducting pellets. Superconductor Science and Technology, 1997, 10, 147-155.  | 1.8  | 58        |
| 176 | Fine Strontium Ferrite Powders from an Ethanolâ€Based Microemulsion. Journal of the American<br>Ceramic Society, 2000, 83, 1049-1055.  | 1.9  | 58        |
| 177 | Labile Ferroelastic Nanodomains in Bilayered Ferroelectric Thin Films. Advanced Materials, 2009, 21, 3497-3502.  | 11.1 | 58        |
| 178 | MOFâ€Derived Vertically Aligned Mesoporous Co <sub>3</sub> O <sub>4</sub> Nanowires for Ultrahigh<br>Capacity Lithiumâ€lon Batteries Anodes. Advanced Materials Interfaces, 2018, 5, 1800222.                  | 1.9  | 58        |
| 179 | Microstructural Origins of High Piezoelectric Performance: A Pathway to Practical Leadâ€Free<br>Materials. Advanced Functional Materials, 2019, 29, 1902911.   | 7.8  | 58        |
| 180 | Epsilon-negative BaTiO3/Cu composites with high thermal conductivity and yet low electrical conductivity. Journal of Materiomics, 2020, 6, 145-151.  | 2.8  | 58        |

| #   | Article  | IF   | CITATIONS |
|-----|--|------|-----------|
| 181 | Nanosized Barium Titanate Powder by Mechanical Activation. Journal of the American Ceramic Society, 2000, 83, 232-34.  | 1.9  | 57        |
| 182 | Ferroelectricity and ferroelectric resistive switching in sputtered Hf0.5Zr0.5O2 thin films. Applied Physics Letters, 2016, 108, .   | 1.5  | 57        |
| 183 | Twinned Tungsten Carbonitride Nanocrystals Boost Hydrogen Evolution Activity and Stability. Small, 2019, 15, e1900248.   | 5.2  | 57        |
| 184 | Electrospun Nanofibers for New Generation Flexible Energy Storage. Energy and Environmental<br>Materials, 2021, 4, 502-521.  | 7.3  | 57        |
| 185 | Rice husk-derived Mn <sub>3</sub> O <sub>4</sub> /manganese silicate/C nanostructured composites for high-performance hybrid supercapacitors. Inorganic Chemistry Frontiers, 2019, 6, 2788-2800. | 3.0  | 56        |
| 186 | Flexible and Wearable All-Solid-State Al–Air Battery Based on Iron Carbide Encapsulated in<br>Electrospun Porous Carbon Nanofibers. ACS Applied Materials & Interfaces, 2019, 11, 1988-1995.     | 4.0  | 56        |
| 187 | Ultrafine Barium Titanate Powders via Microemulsion Processing Routes. Journal of the American<br>Ceramic Society, 1999, 82, 873-881.  | 1.9  | 55        |
| 188 | Thickness and coupling effects in bilayered multiferroic CoFe2O4/Pb(Zr0.52Ti0.48)O3 thin films.<br>Journal of Applied Physics, 2008, 103, .  | 1.1  | 55        |
| 189 | Facile synthesis of hybrid silica nanocapsules by interfacial templating condensation and their application in fluorescence imaging. Chemical Communications, 2009, , 6240.                      | 2.2  | 55        |
| 190 | High-performance B4C–TiB2–SiC composites with tuneable properties fabricated by reactive hot pressing. Journal of the European Ceramic Society, 2019, 39, 2995-3002.                             | 2.8  | 55        |
| 191 | Synergizing aliovalent doping and interface in heterostructured NiV nitride@oxyhydroxide core-shell nanosheet arrays enables efficient oxygen evolution. Nano Energy, 2021, 85, 105961.          | 8.2  | 55        |
| 192 | Swapping Catalytic Active Sites from Cationic Ni to Anionic S in Nickel Sulfide Enables More Efficient<br>Alkaline Hydrogen Generation. Advanced Energy Materials, 2022, 12, .                   | 10.2 | 55        |
| 193 | Silica-shell cross-linked micelles encapsulating fluorescent conjugated polymers for targeted cellular imaging. Biomaterials, 2012, 33, 237-246.   | 5.7  | 54        |
| 194 | Metal–Organic Frameworks (MOFs)-boosted filtration membrane technology for water sustainability.<br>APL Materials, 2020, 8, .  | 2.2  | 54        |
| 195 | Evolution from Leadâ€Based to Leadâ€Free Piezoelectrics: Engineering of Lattices, Domains, Boundaries, and Defects Leading to Giant Response. Advanced Materials, 2022, 34, e2106845.            | 11.1 | 54        |
| 196 | Strong Charge Transfer at 2H–1T Phase Boundary of MoS <sub>2</sub> for Superb Highâ€Performance<br>Energy Storage. Small, 2019, 15, e1900131.  | 5.2  | 53        |
| 197 | Recent advances and future perspectives for graphene oxide reinforced epoxy resins. Materials Today<br>Communications, 2020, 23, 100883.   | 0.9  | 53        |
| 198 | 3D-printed surface-patterned ceramic membrane with enhanced performance in crossflow filtration.<br>Journal of Membrane Science, 2020, 606, 118138.  | 4.1  | 53        |

JOHN WANG

| #   | Article  | IF  | CITATIONS |
|-----|--|-----|-----------|
| 199 | Microemulsion processing of manganese zinc ferrites. Materials Letters, 1997, 30, 217-221.   | 1.3 | 52        |
| 200 | Supramolecular-Templated Thick Mesoporous Titania Films for Dye-Sensitized Solar Cells: Effect of Morphology on Performance. ACS Applied Materials & Interfaces, 2009, 1, 2789-2795.                             | 4.0 | 52        |
| 201 | Ferroelectric Behavior in Bismuth Ferrite Thin Films of Different Thickness. ACS Applied Materials<br>& Interfaces, 2011, 3, 3261-3263.  | 4.0 | 52        |
| 202 | (Ba, Ca)(Ti, Zr)O3-BiFeO3 lead-free piezoelectric ceramics. Current Applied Physics, 2012, 12, 534-538.  | 1.1 | 52        |
| 203 | A novel hollowed CoO-in-CoSnO <sub>3</sub> nanostructure with enhanced lithium storage capabilities. Nanoscale, 2014, 6, 13824-13830.  | 2.8 | 52        |
| 204 | Heterogeneous ZIF-L membranes with improved hydrophilicity and anti-bacterial adhesion for potential application in water treatment. RSC Advances, 2019, 9, 1591-1601.   | 1.7 | 51        |
| 205 | Robust pure copper framework by extrusion 3D printing for advanced lithium metal anodes. Journal of<br>Materials Chemistry A, 2020, 8, 9058-9067.  | 5.2 | 51        |
| 206 | Transparent magnetic composites of ZnFe2O4 nanoparticles in silica. Journal of Applied Physics, 2001, 90, 4169-4174.   | 1.1 | 50        |
| 207 | Mesocrystals as a class of multifunctional materials. CrystEngComm, 2014, 16, 5948-5967.   | 1.3 | 50        |
| 208 | Cu and Co nanoparticle-Co-decorated N-doped graphene nanosheets: a high efficiency bifunctional<br>electrocatalyst for rechargeable Zn–air batteries. Journal of Materials Chemistry A, 2019, 7,<br>12851-12858. | 5.2 | 50        |
| 209 | Chemical-grafting of graphene oxide quantum dots (GOQDs) onto ceramic microfiltration membranes for enhanced water permeability and anti-organic fouling potential. Applied Surface Science, 2020, 502, 144128.  | 3.1 | 50        |
| 210 | Nanocomposites of ZnFe2O4 in silica: synthesis, magnetic and optical properties. Materials Chemistry and Physics, 2002, 75, 181-185.   | 2.0 | 49        |
| 211 | The effects of anodization parameters on titania nanotube arrays and dye sensitized solar cells.<br>Nanotechnology, 2008, 19, 405701.  | 1.3 | 49        |
| 212 | A Method to Improve Electrical Properties of BiFeO <sub>3</sub> Thin Films. ACS Applied Materials<br>& Interfaces, 2012, 4, 1182-1185.   | 4.0 | 49        |
| 213 | Hydrothermal growth and optical properties of Nb <sub>2</sub> O <sub>5</sub> nanorod arrays.<br>Journal of Materials Chemistry C, 2014, 2, 8185-8190.  | 2.7 | 49        |
| 214 | Health Promotion Board–Ministry of Health Clinical Practice Guidelines: Obesity. Singapore Medical<br>Journal, 2015, 57, 292-300.  | 0.3 | 49        |
| 215 | Assembling of Bi atoms on TiO <sub>2</sub> nanorods boosts photoelectrochemical water splitting of semiconductors. Nanoscale, 2020, 12, 4302-4308.   | 2.8 | 49        |
| 216 | Developing better ceramic membranes for water and wastewater Treatment: Where microstructure integrates with chemistry and functionalities. Chemical Engineering Journal, 2022, 428, 130456.                     | 6.6 | 49        |

| #   | Article  | IF   | CITATIONS |
|-----|--|------|-----------|
| 217 | Highly efficient dyeâ€sensitized solar cells using phenothiazine derivative organic dyes. Progress in<br>Photovoltaics: Research and Applications, 2010, 18, 573-581.  | 4.4  | 48        |
| 218 | A new class of solid state ionic conductors for application in all solid state dye sensitized solar cells. Chemical Communications, 2010, 46, 2091.  | 2.2  | 48        |
| 219 | Hypophosphite hybrid perovskites: a platform for unconventional tilts and shifts. Chemical Communications, 2018, 54, 3751-3754.  | 2.2  | 48        |
| 220 | A sacrificial Zn strategy enables anchoring of metal single atoms on the exposed surface of holey 2D<br>molybdenum carbide nanosheets for efficient electrocatalysis. Journal of Materials Chemistry A, 2020,<br>8, 3071-3082. | 5.2  | 48        |
| 221 | Improved ferroelectric behavior in (110) oriented BiFeO3 thin films. Journal of Applied Physics, 2010, 107, 034103.  | 1.1  | 47        |
| 222 | All-solid-state sponge-like squeezable zinc-air battery. Energy Storage Materials, 2019, 23, 375-382.  | 9.5  | 47        |
| 223 | Quasi-solid-state fiber-shaped aqueous energy storage devices: recent advances and prospects. Journal of Materials Chemistry A, 2020, 8, 6406-6433.  | 5.2  | 47        |
| 224 | Effects of SRO Buffer Layer on Multiferroic BiFeO <sub>3</sub> Thin Films. Journal of the American Ceramic Society, 2008, 91, 3240-3244.   | 1.9  | 46        |
| 225 | Diodelike and resistive hysteresis behavior of heterolayered BiFeO3/ZnO ferroelectric thin films.<br>Journal of Applied Physics, 2010, 108, .  | 1.1  | 46        |
| 226 | A giant polarization value of Zn and Mn co-modified bismuth ferrite thin films. Applied Physics Letters, 2013, 102, .  | 1.5  | 46        |
| 227 | Cobalt monoxide-doped porous graphitic carbon microspheres for supercapacitor application.<br>Scientific Reports, 2013, 3, 2925.   | 1.6  | 46        |
| 228 | Quench-tailored Al-doped V2O5 nanomaterials for efficient aqueous zinc-ion batteries. Journal of<br>Energy Chemistry, 2022, 70, 52-58.   | 7.1  | 46        |
| 229 | Overoxidized Poly{pyrrole-co-[3-(pyrrol-1-yl)- propanesulfonate]}-coated Platinum Electrodes for Selective Detection of Catecholamine Neurotransmitters. Analyst, The, 1997, 122, 981-984.                                     | 1.7  | 45        |
| 230 | Mechanochemically Synthesized Lead Magnesium Niobate. Journal of the American Ceramic Society, 1999, 82, 1358-1360.  | 1.9  | 45        |
| 231 | Phase transitions and electrical behavior of lead-free (K0.50Na0.50)NbO3 thin film. Journal of Applied Physics, 2009, 106, .   | 1.1  | 45        |
| 232 | Nanohollow Carbon for Rechargeable Batteries: Ongoing Progresses and Challenges. Nano-Micro<br>Letters, 2020, 12, 183.   | 14.4 | 45        |
| 233 | Mechanochemical synthesis of nanosized lead titanate powders from mixed oxides. Materials Letters,<br>1999, 39, 364-369.   | 1.3  | 44        |
| 234 | Phase transition, ferroelectric behaviors and domain structures of (Na1/2Bi1/2)1â^'xTiPbxO3 thin films.<br>Acta Materialia, 2006, 54, 1691-1698.   | 3.8  | 44        |

| #   | Article  | IF   | CITATIONS |
|-----|--|------|-----------|
| 235 | Ferroelectricity emerging in strained (111)-textured ZrO2 thin films. Applied Physics Letters, 2016, 108, .  | 1.5  | 44        |
| 236 | From Well-Defined Carbon-Rich Precursors to Monodisperse Carbon Particles with Hierarchic Structures. Advanced Materials, 2007, 19, 1849-1853.   | 11.1 | 43        |
| 237 | Toughening mechanisms in duplex alumina-zirconia ceramics. Journal of Materials Science, 1988, 23, 804-808.  | 1.7  | 42        |
| 238 | Highly dispersed gold nanoparticles assembled in mesoporous titania films of cubic configuration.<br>Microporous and Mesoporous Materials, 2008, 110, 242-249.   | 2.2  | 42        |
| 239 | ZnO as a buffer layer for growth of BiFeO3 thin films. Journal of Applied Physics, 2010, 108, .  | 1.1  | 42        |
| 240 | Tuning the porous texture and specific surface area of nanoporous carbons for supercapacitor<br>electrodes by adjusting the hydrothermal synthesis temperature. Journal of Materials Chemistry A,<br>2013, 1, 12962. | 5.2  | 42        |
| 241 | Microwave – assisted hydrothermal synthesis of nanocrystal β-Ni(OH) <sub>2</sub> for supercapacitor applications. CrystEngComm, 2016, 18, 3256-3264.   | 1.3  | 42        |
| 242 | Open hollow Co–Pt clusters embedded in carbon nanoflake arrays for highly efficient alkaline water splitting. Journal of Materials Chemistry A, 2018, 6, 20214-20223.  | 5.2  | 42        |
| 243 | Electronic-reconstruction-enhanced hydrogen evolution catalysis in oxide polymorphs. Nature<br>Communications, 2019, 10, 3149.   | 5.8  | 42        |
| 244 | Effect of gradient profile in ceramic membranes on filtration characteristics: Implications for membrane development. Journal of Membrane Science, 2020, 595, 117576.  | 4.1  | 42        |
| 245 | Flexible quasi-solid-state aqueous Zn-based batteries: rational electrode designs for<br>high-performance and mechanical flexibility. Materials Today Energy, 2020, 18, 100523.                                      | 2.5  | 42        |
| 246 | Fabrication of 3D-Printed Ceramic Structures for Portable Solar Desalination Devices. ACS Applied Materials & Interfaces, 2021, 13, 23220-23229.   | 4.0  | 42        |
| 247 | Dramatic effect of a small amount of MgO addition on the sintering of Al2O3-5 vol% SiC nanocomposite. Materials Letters, 1998, 33, 273-277.  | 1.3  | 41        |
| 248 | Raman and magnetization studies of barium ferrite powder prepared by water-in-oil microemulsion.<br>Journal of Materials Research, 2000, 15, 483-487.  | 1.2  | 41        |
| 249 | Hydrothermal Growth of Vertical ZnO Nanorods. Journal of the American Ceramic Society, 2009, 92, 1940-1945.  | 1.9  | 41        |
| 250 | Near-infrared emission from Eu–Yb doped silicate glasses subjected to thermal reduction. Applied<br>Physics Letters, 2011, 98, .   | 1.5  | 41        |
| 251 | Structural and topological aspects of borophosphate glasses and their relation to physical properties. Journal of Chemical Physics, 2015, 142, 184503.   | 1.2  | 41        |
| 252 | Relaxivity and toxicological properties of manganese oxide nanoparticles for MRI applications. RSC<br>Advances, 2016, 6, 45462-45474.  | 1.7  | 41        |

| #   | Article   | IF  | CITATIONS |
|-----|---|-----|-----------|
| 253 | Efficient Water Splitting System Enabled by Multifunctional Platinumâ€Free Electrocatalysts. Advanced<br>Functional Materials, 2021, 31, 2009853.   | 7.8 | 41        |
| 254 | Designing Poly[( <i>R</i> )-3-hydroxybutyrate]-Based Polyurethane Block Copolymers for Electrospun<br>Nanofiber Scaffolds with Improved Mechanical Properties and Enhanced Mineralization Capability.<br>Journal of Physical Chemistry B, 2010, 114, 7489-7498. | 1.2 | 40        |
| 255 | Growth rate induced monoclinic to tetragonal phase transition in epitaxial BiFeO3 (001) thin films.<br>Applied Physics Letters, 2011, 98, 102902.   | 1.5 | 40        |
| 256 | Nanoparticle morphology and film-forming behavior of polyacrylate/ZnO nanocomposite. Composites Science and Technology, 2014, 98, 64-71.  | 3.8 | 40        |
| 257 | Silica–F127 nanohybrid-encapsulated manganese oxide nanoparticles for optimized<br>T <sub>1</sub> magnetic resonance relaxivity. Nanoscale, 2014, 6, 293-299.   | 2.8 | 40        |
| 258 | pHâ€Activatable MnOâ€Based Fluorescence and Magnetic Resonance Bimodal Nanoprobe for Cancer<br>Imaging. Advanced Healthcare Materials, 2016, 5, 721-729.  | 3.9 | 40        |
| 259 | Photosynthetic apparatus of Rhodobacter sphaeroides exhibits prolonged charge storage. Nature Communications, 2019, 10, 902.  | 5.8 | 40        |
| 260 | A negative-feedback loop maintains optimal chemokine concentrations for directional cell migration.<br>Nature Cell Biology, 2020, 22, 266-273.  | 4.6 | 40        |
| 261 | Fabrication and microstructure-mechanical property relationships in Ce-TZPs. Journal of Materials Science, 1992, 27, 5348-5356.   | 1.7 | 39        |
| 262 | A Bicontinuous Microemulsion Route to Zinc Oxide Powder. Ceramics International, 1998, 24, 205-209.   | 2.3 | 39        |
| 263 | Heterolayered lead zirconate titanate thin films of giant polarization. Journal of Applied Physics, 2004, 96, 5706-5711.  | 1.1 | 39        |
| 264 | Single atom catalysts: a surface heterocompound perspective. Nanoscale Horizons, 2020, 5, 757-764.  | 4.1 | 39        |
| 265 | Leakage current and charge carriers in (Na0.5Bi0.5)TiO3thin film. Journal Physics D: Applied Physics, 2005, 38, 642-648.  | 1.3 | 38        |
| 266 | Charged defects and their effects on electrical behavior in Bi1â^'xLaxFeO3 thin films. Journal of Applied Physics, 2009, 105, 016106.   | 1.1 | 38        |
| 267 | Impedance spectroscopy of bilayered bismuth ferrite thin films. Journal of Applied Physics, 2011, 110, .  | 1.1 | 38        |
| 268 | Stable Ferroelectric Perovskite Structure with Giant Axial Ratio and Polarization in Epitaxial<br>BiFe <sub>0.6</sub> Ga <sub>0.4</sub> O <sub>3</sub> Thin Films. ACS Applied Materials & Interfaces,<br>2015, 7, 2648-2653.                                   | 4.0 | 38        |
| 269 | Low-loss and temperature-stable negative permittivity in La0.5Sr0.5MnO3 ceramics. Journal of the European Ceramic Society, 2020, 40, 1917-1921.   | 2.8 | 38        |
| 270 | Quenchâ€Induced Surface Engineering Boosts Alkaline Freshwater and Seawater Oxygen Evolution<br>Reaction of Porous NiCo <sub>2</sub> O <sub>4</sub> Nanowires. Small, 2022, 18, e2106187.   | 5.2 | 38        |

| #   | Article   | IF   | CITATIONS |
|-----|---|------|-----------|
| 271 | Degradable Cross-Linked Collagen Fiber/MXene Composite Aerogels as a High-Performing Sensitive<br>Pressure Sensor. ACS Sustainable Chemistry and Engineering, 2022, 10, 1408-1418.  | 3.2  | 38        |
| 272 | The effects of notch width on the SENB toughness for oxide ceramics. Journal of the European Ceramic Society, 1992, 10, 21-31.  | 2.8  | 37        |
| 273 | Mechanochemical fabrication of single phase PMN of perovskite structure. Solid State Ionics, 1999, 124, 271-279.  | 1.3  | 37        |
| 274 | Mechanochemical Synthesis of 0.9 Pb(Mg1/3Nb2/3)O3-0.1 PbTiO3from Mixed Oxides. Advanced Materials, 1999, 11, 210-213.   | 11.1 | 37        |
| 275 | Effect of high-energy mechanical activation on the microstructure and electrical properties of ZnO-based varistors. Solid State Ionics, 2000, 132, 107-117.   | 1.3  | 37        |
| 276 | Twinning rotation and ferroelectric behavior of epitaxial BiFeO3 (001) thin film. Applied Physics<br>Letters, 2010, 96, .   | 1.5  | 37        |
| 277 | Enhanced photovoltaic effects and switchable conduction behavior in BiFe0.6Sc0.4O3 thin films. Acta<br>Materialia, 2015, 88, 83-90.   | 3.8  | 37        |
| 278 | Hydrogenated TiO2 membrane with photocatalytically enhanced anti-fouling for ultrafiltration of surface water. Applied Catalysis B: Environmental, 2020, 264, 118528.   | 10.8 | 37        |
| 279 | How different is mechanical activation from thermal activation? A case study with PZN and PZN-based relaxors. Solid State Ionics, 2000, 127, 169-175.   | 1.3  | 36        |
| 280 | In vitro bioactivity assessment of 70 (wt.)%SiO2–30 (wt.)%CaO bioactive glasses in simulated body<br>fluid. Materials Letters, 2005, 59, 3267-3271.   | 1.3  | 36        |
| 281 | Probing the Microporous Structure of Silica Shell Via Aggregationâ€Induced Emission in<br>Au(I)â€Thiolate@SiO <sub>2</sub> Nanoparticle. Small, 2016, 12, 6537-6541.  | 5.2  | 36        |
| 282 | Hollow structure engineering of FeCo alloy nanoparticles electrospun in nitrogen-doped carbon<br>enables high performance flexible all-solid-state zinc–air batteries. Sustainable Energy and Fuels,<br>2020, 4, 1747-1753. | 2.5  | 36        |
| 283 | Fabricating densified hydroxyapatite ceramics from a precipitated precursor. Materials Letters, 1999, 38, 208-213.  | 1.3  | 35        |
| 284 | Ultrafine zinc oxide powders prepared by precipitation/mechanical milling. Journal of Materials<br>Science, 2001, 36, 3273-3276.  | 1.7  | 35        |
| 285 | Phosphorusâ€Based Electrocatalysts: Black Phosphorus, Metal Phosphides, and Phosphates. Advanced<br>Materials Interfaces, 2020, 7, 2000676.   | 1.9  | 35        |
| 286 | Manipulating Interfaces of Electrocatalysts Down to Atomic Scales: Fundamentals, Strategies, and<br>Electrocatalytic Applications. Small Methods, 2021, 5, e2001010.  | 4.6  | 35        |
| 287 | Reduced crystallization temperature in a microemulsion-derived zirconia precursor. Materials<br>Letters, 1997, 30, 119-124.   | 1.3  | 34        |
| 288 | Comparative study on phase development of lead titanate powders. Materials Letters, 2002, 52, 304-312.  | 1.3  | 34        |

| #   | Article   | IF                   | CITATIONS |
|-----|---|----------------------|-----------|
| 289 | Origin of the enhanced polarization in La and Mg co-substituted BiFeO3 thin film during the fatigue process. Applied Physics Letters, 2012, 100, .  | 1.5                  | 34        |
| 290 | Overcoming the Limits of the Interfacial Dzyaloshinskii–Moriya Interaction by Antiferromagnetic<br>Order in Multiferroic Heterostructures. Advanced Materials, 2020, 32, e1904415.  | 11.1                 | 34        |
| 291 | Ultrafine zirconia powders via microemulsion processing route. Scripta Materialia, 1997, 8, 499-505.  | 0.5                  | 33        |
| 292 | Mechanochemical Synthesis of Hydroxyapatite from Calcium Oxide and Brushite. Journal of the<br>American Ceramic Society, 2001, 84, 465-67.  | 1.9                  | 33        |
| 293 | A Hybrid Silica Nanoreactor Framework for Encapsulation of Hollow Manganese Oxide Nanoparticles<br>of Superior T <sub>1</sub> Magnetic Resonance Relaxivity. Advanced Functional Materials, 2015, 25,<br>5269-5276.   | 7.8                  | 33        |
| 294 | 3D hierarchical SnO <sub>2</sub> @Ni(OH) <sub>2</sub> core–shell nanowire arrays on carbon cloth<br>for energy storage application. Journal of Materials Chemistry A, 2015, 3, 9538-9542.   | 5.2                  | 33        |
| 295 | Large-area multifunctional electro-chromic-chemical device made of W17O47 nanowires by Zn2+ ion intercalation. Nano Energy, 2021, 89, 106356.   | 8.2                  | 33        |
| 296 | Thickness-dependent twinning evolution and ferroelectric behavior of epitaxial <mml:math<br>xmlns:mml="http://www.w3.org/1998/Math/MathML"<br/>display="inline"&gt;<mml:mrow><mml:msub><mml:mrow><mml:mtext>BiFeO</mml:mtext></mml:mrow><mml:n<br>thin films. Physical Review B, 2010, 82, .</mml:n<br></mml:msub></mml:mrow></mml:math<br> | n> <sup>11</sup> /mn | ו:mn>     |
| 297 | Synthesis of Pb(Mg <sub>1/3</sub> Nb <sub>2/3</sub> )O <sub>3</sub> in Excess Lead Oxide by Mechanical Activation. Journal of the American Ceramic Society, 2001, 84, 660-662.  | 1.9                  | 31        |
| 298 | Dielectric relaxation in SrBi2(V0.1Nb0.9)2O9 layered perovskite ceramics. Materials Chemistry and Physics, 2002, 75, 50-55.   | 2.0                  | 31        |
| 299 | Functional ceramics of nanocrystallinity by mechanical activation. Solid State Ionics, 2002, 151, 403-412.  | 1.3                  | 31        |
| 300 | Modulated charged defects and conduction behaviour in doped BiFeO <sub>3</sub> thin films. Journal<br>Physics D: Applied Physics, 2009, 42, 162001.   | 1.3                  | 31        |
| 301 | 0.90(Na0.5Bi0.5TiO3)-0.06BaTiO3-0.04K0.5Na0.5NbO3 Ferroelectric Thin Films Derived from Chemical Solutions. Journal of the American Ceramic Society, 2011, 94, 1331-1335.   | 1.9                  | 31        |
| 302 | Growth of centimeter-sized<br>[(CH <sub>3</sub> ) <sub>2</sub> NH <sub>2</sub> ][Mn(HCOO) <sub>3</sub> ] hybrid formate perovskite<br>single crystals and Raman evidence of pressure-induced phase transitions. New Journal of Chemistry,<br>2017, 41, 151-159.   | 1.4                  | 31        |
| 303 | Free-Standing Black Phosphorus Thin Films for Flexible Quasi-Solid-State Micro-Supercapacitors with<br>High Volumetric Power and Energy Density. ACS Applied Materials & Interfaces, 2019, 11, 5938-5946.   | 4.0                  | 31        |
| 304 | Mechanicalâ€Activationâ€Triggered Gibbsiteâ€ŧoâ€Boehmite Transition and Activationâ€Derived Alumina<br>Powders. Journal of the American Ceramic Society, 2001, 84, 1225-1230.   | 1.9                  | 30        |
| 305 | Bismuth Titanate from Mechanical Activation of a Chemically Coprecipitated Precursor. Journal of the American Ceramic Society, 2002, 85, 2660-2665.   | 1.9                  | 30        |
| 306 | Titania-PMMA nanohybrids of enhanced nanocrystallinity. Journal of Electroceramics, 2006, 16, 431-439.  | 0.8                  | 30        |

JOHN WANG

| #   | Article  | IF                 | CITATIONS                |
|-----|--|--------------------|--------------------------|
| 307 | Ferroelectric and dielectric behavior of heterolayered PZT thin films. Journal of Applied Physics, 2007, 102, .  | 1.1                | 30                       |
| 308 | The effects of ethyl cellulose on PV performance of DSSC made of nanostructured ZnO pastes. Thin Solid Films, 2010, 518, e68-e71.  | 0.8                | 30                       |
| 309 | Ferroelastic domain wall dynamics in ferroelectric bilayers. Acta Materialia, 2010, 58, 5316-5325.   | 3.8                | 30                       |
| 310 | Bipolar and unipolar electrical fatigue in ferroelectric lead zirconate titanate thin films: An experimental comparison study. Journal of Applied Physics, 2010, 108, .  | 1.1                | 30                       |
| 311 | Doping cobalt hydroxide nanowires for better supercapacitor performance. Acta Materialia, 2015, 84, 20-28.   | 3.8                | 30                       |
| 312 | (K,Na)NbO <sub>3</sub> Nanofiber-based Self-Powered Sensors for Accurate Detection of Dynamic<br>Strain. ACS Applied Materials & Interfaces, 2015, 7, 4921-4927.   | 4.0                | 29                       |
| 313 | Confined Fe <sub>2</sub> O <sub>3</sub> Nanoparticles on Graphite Foam as Highâ€Rate and Stable<br>Lithiumâ€ion Battery Anode. Particle and Particle Systems Characterization, 2016, 33, 487-492.  | 1.2                | 29                       |
| 314 | Facile Synthesis of Chitosan-Coated Silica Nanocapsules via Interfacial Condensation Approach for<br>Sustained Release of Vanillin. Industrial & Engineering Chemistry Research, 2018, 57, 6171-6179.                                      | 1.8                | 29                       |
| 315 | Progress and prospects of aberration-corrected STEM for functional materials. Ultramicroscopy, 2018, 194, 182-192.   | 0.8                | 29                       |
| 316 | Activating inverse spinel NiCo2O4 embedded in N-doped carbon nanofibers via Fe substitution for bifunctional oxygen electrocatalysis. Materials Today Physics, 2021, 17, 100353.   | 2.9                | 29                       |
| 317 | Quasiâ€Paired Pt Atomic Sites on Mo <sub>2</sub> C Promoting Selective Fourâ€Electron Oxygen<br>Reduction. Advanced Science, 2021, 8, e2101344.  | 5.6                | 29                       |
| 318 | Sequential Combination of Constituent Oxides in the Synthesis of<br>Pb(Fe <sub>1/2</sub> Nb <sub>1/2</sub> )O <sub>3</sub> by Mechanical Activation. Journal of the<br>American Ceramic Society, 2002, 85, 565-572.                        | 1.9                | 28                       |
| 319 | Ferroelectric behaviors and charge carriers in Nd-doped Bi4Ti3O12 thin films. Journal of Applied Physics, 2005, 97, 034101.  | 1.1                | 28                       |
| 320 | (1Ââ^'Â <i>x</i> ) <scp><scp>Ba</scp>(/scp&gt;(<scp>Zr</scp><sub>0.2</sub><scp>Ti</scp><sub>0.8</sub><br/>Ferroelectric Thin Films Prepared from Chemical Solutions. Journal of the American Ceramic Society,<br/>2012, 95, 986-991.</scp> | ) <s<br>1.9</s<br> | scp> <scp>O<br/>28</scp> |
| 321 | Silica Nanocapsules of Fluorescent Conjugated Polymers and Superparamagnetic Nanocrystals for<br>Dualâ€Mode Cellular Imaging. Chemistry - A European Journal, 2011, 17, 6696-6706.   | 1.7                | 28                       |
| 322 | Valence-driven electrical behavior of manganese-modified bismuth ferrite thin films. Journal of Applied Physics, 2011, 109, 124118.  | 1.1                | 28                       |
| 323 | In-situ surface self-reconstruction in ternary transition metal dichalcogenide nanorod arrays<br>enables efficient electrocatalytic oxygen evolution. Journal of Energy Chemistry, 2021, 55, 10-16.  | 7.1                | 28                       |
| 324 | Single metal atoms catalysts—Promising candidates for next generation energy storage and conversion devices. EcoMat, 2022, 4, .  | 6.8                | 28                       |

| #   | Article  | IF   | CITATIONS |
|-----|--|------|-----------|
| 325 | Zincophilic 3D ZnOHF nanowire arrays with ordered and continuous Zn2+ Ion modulation layer enable long-term stable Zn metal anodes. Energy Storage Materials, 2022, 50, 435-443.   | 9.5  | 28        |
| 326 | Surface toughening of TZP ceramics by low temperature ageing. Ceramics International, 1989, 15, 15-21.   | 2.3  | 27        |
| 327 | Preparation and characterisation of ultrafine lead titanate (PbTiO3) powders. Journal of Materials<br>Science, 1999, 34, 1943-1952.  | 1.7  | 27        |
| 328 | Uniaxial strain-induced ferroelectric phase with a giant axial ratio in a (110) BiFeO <mml:math<br>xmlns:mml="http://www.w3.org/1998/Math/MathML" display="inline"&gt;<mml:msub><mml:mrow<br>/&gt;<mml:mn>3</mml:mn></mml:mrow<br></mml:msub>thin film. Physical Review B, 2013, 87, .</mml:math<br> | 1.1  | 27        |
| 329 | Structural Instability of Epitaxial (001) BiFeO3 Thin Films under Tensile Strain. Scientific Reports, 2014,<br>4, 4631.  | 1.6  | 27        |
| 330 | The Atomic Circus: Small Electron Beams Spotlight Advanced Materials Down to the Atomic Scale.<br>Advanced Materials, 2018, 30, e1802402.  | 11.1 | 27        |
| 331 | Interfacial diffusion assisted chemical deposition (ID-CD) for confined surface modification of alumina microfiltration membranes toward high-flux and anti-fouling. Separation and Purification Technology, 2020, 235, 116177.  | 3.9  | 27        |
| 332 | The effects of mechanical activation in synthesizing ultrafine barium ferrite powders from co-precipitated precursors. Journal of Materials Chemistry, 2000, 10, 1745-1749.  | 6.7  | 26        |
| 333 | Unipolar and bipolar fatigue in antiferroelectric lead zirconate thin films and evidences for switching-induced charge injection inducing fatigue. Applied Physics Letters, 2010, 96, .  | 1.5  | 26        |
| 334 | Anosmin1 Shuttles Fgf to Facilitate Its Diffusion, Increase Its Local Concentration, and Induce Sensory<br>Organs. Developmental Cell, 2018, 46, 751-766.e12.  | 3.1  | 26        |
| 335 | Nanodiamond decorated graphene oxide and the reinforcement to epoxy. Composites Science and Technology, 2018, 165, 9-17.   | 3.8  | 26        |
| 336 | Overcoming the Trade-off between Water Permeation and Mechanical Strength of Ceramic Membrane Supports by Interfacial Engineering. ACS Applied Materials & amp; Interfaces, 2021, 13, 29199-29211.   | 4.0  | 26        |
| 337 | Ceramic-Polymer Composite Membranes for Water and Wastewater Treatment: Bridging the Big Gap<br>between Ceramics and Polymers. Molecules, 2021, 26, 3331.  | 1.7  | 26        |
| 338 | <scp>Threeâ€dimensional</scp> knotting of<br><scp>W<sub>17</sub>O<sub>47</sub></scp> @ <scp>PEDOT</scp> : <scp>PSS</scp> nanowires enables<br><scp>highâ€performance</scp> flexible cathode for dualâ€functional electrochromic and<br>electrochemical device. InformaÄnÃ-MateriÃily, 2022, 4, .     | 8.5  | 26        |
| 339 | Femtosecond third-order optical nonlinearity of BiFeO3. Optics Express, 2009, 17, 10970.   | 1.7  | 25        |
| 340 | MnOx nanosheets for improved electrochemical performances through bilayer nano-architecting.<br>Journal of Power Sources, 2015, 286, 394-399.  | 4.0  | 25        |
| 341 | Controllable structure transitions of Mn <sub>3</sub> O <sub>4</sub> nanomaterials and their effects on electrochemical properties. Nanoscale Horizons, 2017, 2, 326-332.  | 4.1  | 25        |
| 342 | Enhancing water permeation through alumina membranes by changing from cylindrical to conical nanopores. Nanoscale, 2019, 11, 9869-9878.  | 2.8  | 25        |

| #   | Article   | IF  | CITATIONS |
|-----|---|-----|-----------|
| 343 | Unlocking the synergy of interface and oxygen vacancy by core-shell nickel phosphide@oxyhydroxide nanosheets arrays for accelerating alkaline oxygen evolution kinetics. Chemical Engineering Journal, 2021, 425, 131491. | 6.6 | 25        |
| 344 | Direct ink writing of programmable functional siliconeâ€based composites for 4D printing applications.<br>, 2022, 1, 507-516.   |     | 25        |
| 345 | Zirconia toughened cordierite. Journal of Materials Science, 1990, 25, 3982-3989.   | 1.7 | 24        |
| 346 | Synthesis of lead zirconate titanate from an amorphous precursor by mechanical activation. Journal of Alloys and Compounds, 2000, 308, 139-146.   | 2.8 | 24        |
| 347 | Fabrication of YBa2Cu3O7â^'x (YBCO) superconductor bulk structures by extrusion freeforming.<br>Ceramics International, 2016, 42, 15836-15842.  | 2.3 | 24        |
| 348 | MOF-derived manganese oxide/carbon nanocomposites with raised capacitance for stable asymmetric supercapacitor. RSC Advances, 2020, 10, 34403-34412.  | 1.7 | 24        |
| 349 | High temperature piezoelectric strontium bismuth titanate from mechanical activation of mixed oxides. Materials Chemistry and Physics, 2002, 75, 131-135.   | 2.0 | 23        |
| 350 | Layer structured calcium bismuth titanate by mechanical activation. Materials Letters, 2004, 58, 2032-2036.   | 1.3 | 23        |
| 351 | Fatigue and ferroelectric behavior of La and Zn comodified BiFeO3 thin films. Journal of Applied Physics, 2010, 108, .  | 1.1 | 23        |
| 352 | Effect of manganese doping on the size effect of lead zirconate titanate thin films and the extrinsic nature of †dead layers'. Journal of Physics Condensed Matter, 2010, 22, 055901.                                     | 0.7 | 23        |
| 353 | Formation and Anisotropic Dissolution Behavior of NH <sub>4</sub> TiOF <sub>3</sub> Mesocrystals.<br>Crystal Growth and Design, 2011, 11, 2905-2912.  | 1.4 | 23        |
| 354 | Manipulating the Formation of NH <sub>4</sub> TiOF <sub>3</sub> Mesocrystals: Effects of Temperature, Surfactant, and pH. Crystal Growth and Design, 2012, 12, 2625-2633.   | 1.4 | 23        |
| 355 | Synthesis of Au-SiO <sub>2</sub> Asymmetric Clusters and Their Application in ZnO Nanosheet-Based<br>Dye-Sensitized Solar Cells. ACS Applied Materials & Interfaces, 2013, 5, 5601-5608.                                  | 4.0 | 23        |
| 356 | Controlled growth of a metal–organic framework on gold nanoparticles. CrystEngComm, 2016, 18,<br>5262-5266.   | 1.3 | 23        |
| 357 | Synthesis and Characterization of Silicaâ^'Copper Oxide Composite Derived from Microemulsion Processing. Langmuir, 1999, 15, 3056-3061.   | 1.6 | 22        |
| 358 | Gene delivery to the heart by magnetic nanobeads. Journal of Magnetism and Magnetic Materials, 2007, 311, 336-341.  | 1.0 | 22        |
| 359 | Tunable photoluminescence induced by thermal reduction in rare earth doped glasses. Journal of<br>Materials Chemistry, 2011, 21, 6614.  | 6.7 | 22        |
| 360 | <scp><scp>ZnO</scp></scp> Nanosheets Derived from Surfactantâ€Directed Process: Growth<br>Mechanism, and Application in Dyeâ€Sensitized Solar Cells. Journal of the American Ceramic Society,<br>2012, 95, 1241-1246.     | 1.9 | 22        |

| #   | Article  | IF  | CITATIONS |
|-----|--|-----|-----------|
| 361 | An α–Fe <sub>2</sub> O <sub>3</sub> powder of nanosized particles via precursor dispersion. Journal of Materials Research, 1999, 14, 3355-3362.  | 1.2 | 21        |
| 362 | B-site disordering in Pb(Sc1/2Ta1/2)O3 by mechanical activation. Applied Physics Letters, 2003, 82, 4773-4775.   | 1.5 | 21        |
| 363 | Morphology, Optical, and Magnetic Properties of Zn <sub>1â^'<i>x</i></sub> Co <sub><i>x</i></sub> O<br>Nanorods Grown via a Wet Chemical Route. Journal of the American Ceramic Society, 2010, 93,<br>3798-3802. | 1.9 | 21        |
| 364 | Atomic-layer-deposition alumina induced carbon on porous Ni <sub>x</sub> Co <sub>1 â^' x</sub> O<br>nanonets for enhanced pseudocapacitive and Li-ion storage performance. Nanotechnology, 2015, 26,<br>014001.  | 1.3 | 21        |
| 365 | Hydrazine reduction of LaNiO <sub>3</sub> for active materials in supercapacitors. Journal of the American Ceramic Society, 2017, 100, 4629-4637.  | 1.9 | 21        |
| 366 | Room-temperature H2 gasochromic behavior of Pd-modified MoO3 nanowire labels. Materials<br>Chemistry and Physics, 2019, 227, 111-116.  | 2.0 | 21        |
| 367 | Lead zirconate titanate-barium titanate by mechanical activation of mixed oxides. Applied Physics A:<br>Materials Science and Processing, 1999, 69, 433-436.   | 1.1 | 20        |
| 368 | Significant dielectric enhancement in 0.3BiFeO3–0.7SrBi2Nb2O9. Applied Physics Letters, 2001, 79, 2061-2063.   | 1.5 | 20        |
| 369 | Thickness dependences of ferroelectric and dielectric properties in (Bi3.15Nd0.85)Ti3O12 thin films.<br>Journal of Applied Physics, 2006, 99, 074103.  | 1.1 | 20        |
| 370 | Multiferroic BiFeO3Thin Films Buffered by a SrRuO3Layer. Journal of the American Ceramic Society, 2008, 91, 463-466.   | 1.9 | 20        |
| 371 | Observation of a fifth-order optical nonlinearity in Bi0.9La0.1Fe0.98Mg0.02O3 ferroelectric thin films.<br>Applied Physics Letters, 2009, 95, 041114.  | 1.5 | 20        |
| 372 | Resistive hysteresis in BiFeO3 thin films. Materials Research Bulletin, 2011, 46, 2183-2186.   | 2.7 | 20        |
| 373 | High optical performance and practicality of active plasmonic devices based on rhombohedral BiFeO <sub>3</sub> . Laser and Photonics Reviews, 2012, 6, 684-689.  | 4.4 | 20        |
| 374 | From NH <sub>4</sub> TiOF <sub>3</sub> nanoparticles to<br>NH <sub>4</sub> TiOF <sub>3</sub> mesocrystals: steric hindrance versus hydrophobic attraction of<br>F127 molecules. CrystEngComm, 2013, 15, 791-801. | 1.3 | 20        |
| 375 | Hollow Casein-Based Polymeric Nanospheres for Opaque Coatings. ACS Applied Materials &<br>Interfaces, 2016, 8, 11739-11748.  | 4.0 | 20        |
| 376 | NiFe Layered Double-Hydroxide Nanosheets on a Cactuslike (Ni,Co)Se <sub>2</sub> Support for Water<br>Oxidation. ACS Applied Nano Materials, 2019, 2, 325-333.  | 2.4 | 20        |
| 377 | Surface engineered alumina microfiltration membranes based on rationally constructed core-shell particles. Journal of the European Ceramic Society, 2020, 40, 5951-5958.   | 2.8 | 20        |
| 378 | Fiber-in-tube and particle-in-tube hierarchical nanostructures enable high energy density of<br>MnO2-based asymmetric supercapacitors. Journal of Colloid and Interface Science, 2021, 582, 543-551.             | 5.0 | 20        |

| #   | Article   | IF    | CITATIONS |
|-----|---|-------|-----------|
| 379 | Effects of Chemical Species on the Crystallization Behavior of a Solâ€Derived Zirconia Precursor.<br>Journal of the American Ceramic Society, 1998, 81, 2624-2628.  | 1.9   | 19        |
| 380 | B-site ordering and magnetic behaviours in Ni-doped double perovskite Sr2FeMoO6. Journal Physics D:<br>Applied Physics, 2005, 38, 4003-4008.  | 1.3   | 19        |
| 381 | Ferroelectric and fatigue behavior of Pb(Zr0.52Ti0.48)O3â^•(Bi3.15Nd0.85)Ti3O12 bilayered thin films.<br>Journal of Applied Physics, 2008, 103, 034102.   | 1.1   | 19        |
| 382 | Resistive Hysteresis and Diodelike Behavior of BiFeO[sub 3]/ZnO Heterostructure. Electrochemical and Solid-State Letters, 2010, 13, G9.   | 2.2   | 19        |
| 383 | Multiferroic behavior and electrical conduction of BiFeO3 thin film deposited on quartz substrate.<br>Journal of Alloys and Compounds, 2010, 507, L4-L7.  | 2.8   | 19        |
| 384 | Bendable graphene/conducting polymer hybrid films for freestanding electrodes with high volumetric capacitances. RSC Advances, 2016, 6, 2951-2957.  | 1.7   | 19        |
| 385 | Mixed Xâ€6ite Formate–Hypophosphite Hybrid Perovskites. Chemistry - A European Journal, 2018, 24,<br>11309-11313.   | 1.7   | 19        |
| 386 | Interfacial dielectric layer as an origin of polarization fatigue in ferroelectric capacitors. Scientific<br>Reports, 2020, 10, 7310.   | 1.6   | 19        |
| 387 | Alkali-deficiency driven charged out-of-phase boundaries for giant electromechanical response.<br>Nature Communications, 2021, 12, 2841.  | 5.8   | 19        |
| 388 | Formation and characterization of lead magnesium niobate synthesized from the molten salt of potassium chlorate. Journal of Alloys and Compounds, 1998, 274, 110-117.   | 2.8   | 18        |
| 389 | Residual stress and magnetic behavior of multiferroic CoFe2O4/Pb(Zr0.52Ti0.48)O3 thin films. Journal of Applied Physics, 2009, 105, 084113.   | 1.1   | 18        |
| 390 | Mn4+:BiFeO3/Zn2+:BiFeO3 bilayered thin films of (111) orientation. Applied Surface Science, 2011, 257, 7226-7230.   | 3.1   | 18        |
| 391 | Polyacrylate/Surface-Modified ZnO Nanocomposite as Film-Forming Agent for Leather Finishing.<br>International Journal of Polymeric Materials and Polymeric Biomaterials, 2014, 63, 809-814.   | 1.8   | 18        |
| 392 | Microstructural evolution of charged defects in the fatigue process of polycrystalline BiFeO3 thin films. Acta Materialia, 2015, 82, 190-197.   | 3.8   | 18        |
| 393 | Synthesis and characterization of ultrafine lead zirconate powders. Ceramics International, 1998, 24, 507-513.  | 2.3   | 17        |
| 394 | Processing and Characterization of Microemulsionâ€Derived Lead Magnesium Niobate. Journal of the<br>American Ceramic Society, 1999, 82, 529-536.  | 1.9   | 17        |
| 395 | Improved Ferroelectric and Fatigue Behavior of<br>Bi <sub>0.95</sub> Gd <sub>0.05</sub> FeO <sub>3</sub> /BiFe <sub>0.95</sub> Mn <sub>0.05</sub> O <sub>3&lt;<br/>Bilayered Thin Films. Journal of Physical Chemistry C, 2010, 114, 19318-19321.</sub> | /sub> | 17        |
| 396 | Multiferroic and fatigue behavior of silicon-based bismuth ferrite sandwiched structure. Journal of Materials Chemistry, 2011, 21, 7308.  | 6.7   | 17        |

| #   | Article   | IF   | CITATIONS |
|-----|---|------|-----------|
| 397 | Fundamentals, On-Going Advances and Challenges of Electrochemical Carbon Dioxide Reduction.<br>Electrochemical Energy Reviews, 2022, 5, 82-111.   | 13.1 | 17        |
| 398 | Low temperature synthesis of PZT powders via microemulsion processing. Materials Research<br>Bulletin, 1998, 33, 1045-1055.   | 2.7  | 16        |
| 399 | Synthesis of nanocrystalline γ-Fe2O3 in silica matrix by mechanical crystallization from precursor at room temperature. Materials Chemistry and Physics, 2002, 75, 81-85.   | 2.0  | 16        |
| 400 | Mechanical Activationâ€Assisted Synthesis of Pb(Fe <sub>2/3</sub> W <sub>1/3</sub> )O <sub>3</sub> .<br>Journal of the American Ceramic Society, 2000, 83, 1575-1580.   | 1.9  | 16        |
| 401 | BiFeO <sub>3</sub> Thin Films Deposited on LaNiO <sub>3</sub> â€Buffered SiO <sub>2</sub> /Si Substrate.<br>Journal of the American Ceramic Society, 2010, 93, 1422-1426.   | 1.9  | 16        |
| 402 | A metastable cubic phase of sodium niobate nanoparticles stabilized by chemically bonded solvent molecules. Physical Chemistry Chemical Physics, 2016, 18, 33171-33179.   | 1.3  | 16        |
| 403 | Phospho-oxynitride Layer Protected Cobalt Phosphonitride Nanowire Arrays for High-Rate and Stable<br>Supercapacitors. ACS Applied Energy Materials, 2019, 2, 616-626.   | 2.5  | 16        |
| 404 | Squaraine organic crystals with strong dipole effect toward stable lithium-organic batteries. Energy<br>Storage Materials, 2021, 41, 240-247.   | 9.5  | 16        |
| 405 | Solar-Driven Gas-Phase Moisture to Hydrogen with Zero Bias. ACS Nano, 2021, 15, 19119-19127.  | 7.3  | 16        |
| 406 | One-step synthesis of nitrogen-doped carbon quantum dots for paper-based<br>electrochemiluminescence detection of Cu2+ ions. Microchemical Journal, 2022, 174, 107057.  | 2.3  | 16        |
| 407 | A study of the reaction of Y1Ba2Cu3O7-? superconducting ceramics with water. Journal of Materials Science, 1988, 23, 3393-3397.   | 1.7  | 15        |
| 408 | Synthesis of single phase 0.9Pb[(Zn0.6Mg0.4)1/3Nb2/3O3]–0.1PbTiO3 by mechanically activating mixed oxides. Acta Materialia, 1999, 47, 2283-2291.  | 3.8  | 15        |
| 409 | Ferroelectric properties and leakage current characteristics of radio-frequency-sputtered SrBi2(V0.1Nb0.9)2O9 thin films. Journal of Applied Physics, 2004, 96, 2181-2185.  | 1.1  | 15        |
| 410 | 0.67Pb(Mg1/3Nb2/3)O3–0.33PbTiO3 thin films derived from RF magnetron sputtering. Ceramics<br>International, 2004, 30, 1539-1542.  | 2.3  | 15        |
| 411 | Fatigue behavior of heterostructured Pb(Zr,Ti)O3â^•(Bi,Nd)4Ti3O12 ferroelectric thin films. Applied Physics Letters, 2006, 89, 122905.  | 1.5  | 15        |
| 412 | Hybrid Titania Microspheres of Novel Superstructures Templated by Block Copolymers. Chemistry of<br>Materials, 2011, 23, 2745-2752.   | 3.2  | 15        |
| 413 | Highly (111)-Orientated BiFeO <sub>3</sub> Thin Film Deposited on<br>La <sub>0.67</sub> Sr <sub>0.33</sub> MnO <sub>3</sub> Buffered<br>Pt/TiO <sub>2</sub> /SiO <sub>2</sub> /Si (100) Substrate. Journal of the Electrochemical Society, 2011,<br>159. G11-G14. | 1.3  | 15        |
| 414 | Guided Assembly of Microporous/Mesoporous Manganese Phosphates by Bifunctional<br>Organophosphonic Acid Etching and Templating. Advanced Materials, 2019, 31, e1901124.   | 11.1 | 15        |

JOHN WANG

| #   | Article  | IF                 | CITATIONS             |
|-----|--|--------------------|-----------------------|
| 415 | Polymorphism in M(H <sub>2</sub> PO <sub>2</sub> ) <sub>3</sub> (M = V, Al, Ga) compounds with the perovskite-related ReO <sub>3</sub> structure. Chemical Communications, 2019, 55, 2964-2967.  | 2.2                | 15                    |
| 416 | Combinational Design of Electronic Structure and Nanoarray Architecture Achieves a<br>Lowâ€Overpotential Oxygen Electrode for Aprotic Lithium–Oxygen Batteries. Small Methods, 2020, 4,<br>1900619.  | 4.6                | 15                    |
| 417 | Ultrahigh piezoelectric coefficients of Li-doped (K,Na)NbO3 nanorod arrays with manipulated O-T<br>phase boundary: Towards energy harvesting and self-powered human movement monitoring. Nano<br>Energy, 2021, 86, 106072.                             | 8.2                | 15                    |
| 418 | Preferred ZrO2(t) → ZrO2(m) transformation on the aged surface of TZP ceramics. Journal of Materials<br>Science Letters, 1989, 8, 1195-1198.   | 0.5                | 14                    |
| 419 | Ion-Containing Membranes from Microemulsion Polymerization. Langmuir, 1999, 15, 3202-3205.   | 1.6                | 14                    |
| 420 | Mechanical activation synthesis and dielectric properties of 0.48PFN–0.36PFW–0.16PZN from mixed oxides. Journal of Alloys and Compounds, 2000, 311, 181-187.   | 2.8                | 14                    |
| 421 | Effects of mechanical activation on the formation of PbTiO3 from amorphous Pb–Ti–O precursor.<br>Journal of Applied Physics, 2003, 93, 3470-3474.  | 1.1                | 14                    |
| 422 | Dielectric behaviors of Pb1â^'3x/2LaxTiO3 derived from mechanical activation. Journal of Applied Physics, 2004, 95, 4981-4988.   | 1.1                | 14                    |
| 423 | B‣ite Order–Disorder Transition in<br>Pb(Mg <sub>1/3</sub> Nb <sub>2/3</sub> )O <sub>3</sub> –Pb(Mg <sub>1/2</sub> W <sub>1/2</sub> )O <sub><br/>Triggered by Mechanical Activation. Journal of the American Ceramic Society, 2002, 85, 833-838.</sub> | 3ĸ¢sub>            | 14                    |
| 424 | Inducing Crystallization in an Amorphous Lead Zirconate Titanate Precursor by Mechanical Activation. Journal of the American Ceramic Society, 1999, 82, 1641-1643.   | 1.9                | 14                    |
| 425 | Temperature-dependent electrical behavior of La0.7Sr0.3MnO3-buffered Bi0.9La0.1FeO3 thin films.<br>Journal of Applied Physics, 2009, 106, .  | 1.1                | 14                    |
| 426 | Highly efficient dye-sensitized solar cells of thick mesoporous titania films derived from supramolecular templating. Nanotechnology, 2009, 20, 505602.  | 1.3                | 14                    |
| 427 | Large ZnO Mesocrystals of Hexagonal Columnar Morphology Derived from Liquid Crystal Templates.<br>Journal of the American Ceramic Society, 2011, 94, 3267-3275.  | 1.9                | 14                    |
| 428 | Mechanochemical Synthesis of<br>0.9[0.6Pb(Zn <sub>1/3</sub> Nb <sub>2/3</sub> )O <sub>3</sub> ·0.4Pb(Mg <sub>1/3</sub> Nb <sub>2/3</sub><br>Journal of the American Ceramic Society, 2000, 83, 53-59.  | •) <b>Q9</b> sub>3 | 3⊲ <b>/s</b> ub>]Â∙0. |
| 429 | Nanocrystalline PbTiO3 powders from an amorphous Pb–Ti–O precursor by mechanical activation.<br>Materials Chemistry and Physics, 2002, 75, 216-219.  | 2.0                | 13                    |
| 430 | Nanocrystalline Maghemite (γâ€Fe <sub>2</sub> O <sub>3</sub> ) in Silica by Mechanical Activation of<br>Precursors. Journal of the American Ceramic Society, 2002, 85, 807-811.  | 1.9                | 13                    |
| 431 | Multiferroic behaviour and orientation dependence of lead-free (1) Tj ETQq1 1 0.784314 rgBT /Overlock 10 Tf 50 films. Journal Physics D: Applied Physics, 2009, 42, 195405.  | 107 Td (â´<br>1.3  | ° <i>x</i> )Bi<br>13  |
| 432 | Oxygen-vacancy-mediated negative differential resistance in La and Mg co-substituted BiFeO3 thin film.<br>Journal of Applied Physics, 2011, 110, 124102.   | 1.1                | 13                    |

JOHN WANG

| #   | Article   | IF                | CITATIONS       |
|-----|---|-------------------|-----------------|
| 433 | Extrusion printing of a designed three-dimensional YBa <sub>2</sub> Cu <sub>3</sub> O <sub>7â^'x</sub><br>superconductor with milled precursor powder. Journal of Materials Chemistry C, 2017, 5, 3382-3389.                              | 2.7               | 13              |
| 434 | Nanowires versus nanosheets – Effects of NiCo2O4 nanostructures on ceramic membrane permeability and fouling potential. Separation and Purification Technology, 2019, 215, 644-651.   | 3.9               | 13              |
| 435 | Atomic-Scale Control of Magnetism at the Titanite-Manganite Interfaces. Nano Letters, 2019, 19, 3057-3065.  | 4.5               | 13              |
| 436 | Electrochemiluminescence Detection of Sunset Yellow by Graphene Quantum Dots. Frontiers in Chemistry, 2020, 8, 505.   | 1.8               | 13              |
| 437 | Direct Pyrolysis of a Manganeseâ€Triazolate Metal–Organic Framework into Airâ€Stable Manganese<br>Nitride Nanoparticles. Advanced Science, 2021, 8, 2003212.  | 5.6               | 13              |
| 438 | Aggregation-Induced Luminescence Based UiO-66: Highly Selective Fast-Response Styrene Detection. ACS<br>Applied Materials & Interfaces, 2022, 14, 22510-22520.  | 4.0               | 13              |
| 439 | Synthesis of lead zirconate powders via a polyaniline-mediated microemulsion processing route.<br>Materials Letters, 1998, 36, 179-185.   | 1.3               | 12              |
| 440 | Nanocrystalline Si3N4 with Si–C–N shell structure. Materials Letters, 2001, 49, 318-323.  | 1.3               | 12              |
| 441 | Mechanical activation-induced sequential combination, morphotric segregation and order–disorder transformation in Pb-based relaxors. Materials Science and Engineering B: Solid-State Materials for Advanced Technology, 2003, 99, 63-69. | 1.7               | 12              |
| 442 | Effects of Excess Bi2O3 on the Ferroelectric Behavior of Nd-Doped Bi4Ti3O12 Thin Films. Journal of the<br>American Ceramic Society, 2005, 88, 1037-1040.  | 1.9               | 12              |
| 443 | A theoretical study of permeability enhancement for ultrafiltration ceramic membranes with conical pores and slippage. Physics of Fluids, 2019, 31, .   | 1.6               | 12              |
| 444 | Phase stability and dielectric properties of (1â^'x)PFW+xPZN derived from mechanical activation. Solid State Ionics, 2000, 127, 285-293.  | 1.3               | 11              |
| 445 | Structure characterization of BiFeO3–SrBi2Nb2O9 ceramics by mechanical activation. Materials<br>Science and Engineering B: Solid-State Materials for Advanced Technology, 2003, 99, 116-120.  | 1.7               | 11              |
| 446 | Multiferroic and Fatigue Behavior of (Bi[sub 0.90]La[sub 0.10])FeO[sub 3]/CoFe[sub 2]O[sub 4]/(Bi[sub) Tj ETQq<br>G61.  | 0 0 0 rgBT<br>2.2 | /Overlock<br>11 |
| 447 | BiFeO3/Zn1â^'xMnxO bilayered thin films. Applied Surface Science, 2011, 258, 1390-1394.   | 3.1               | 11              |
| 448 | Combined effects of bilayer structure and ion substitutions on bismuth ferrite thin films. Journal of Applied Physics, 2011, 109, .   | 1.1               | 11              |
| 449 | Ultraviolet photovoltaic effect in BiFeO3/Nb-SrTiO3 heterostructure. Journal of Applied Physics, 2012, 112, .   | 1.1               | 11              |
| 450 | Negative capacitance induced by redistribution of oxygen vacancies in the fatigued BiFeO3-based thin film. Applied Physics Letters, 2012, 101, 022904.  | 1.5               | 11              |

| #   | Article  | IF  | CITATIONS |
|-----|--|-----|-----------|
| 451 | Nickel and Lanthanum Hydroxide Nanocomposites with Much Improved Electrochemical Performance for Supercapacitors. Journal of the American Ceramic Society, 2017, 100, 247-256.   | 1.9 | 11        |
| 452 | Highly permeable Al 2 O 3 microfiltration membranes with holey interior structure achieved through sacrificial C particles. Journal of the American Ceramic Society, 2020, 103, 3361-3372.   | 1.9 | 11        |
| 453 | Ultrathin TiO2 microfiltration membranes supported on a holey intermediate layer to raise filtration performance. Journal of the European Ceramic Society, 2021, 41, 1622-1628.  | 2.8 | 11        |
| 454 | Recent progress in self-supported nanoarrays with diverse substrates for water splitting and beyond.<br>Materials Today Nano, 2021, 15, 100120.  | 2.3 | 11        |
| 455 | Origin of giant electric-field-induced strain in faulted alkali niobate films. Nature Communications, 2022, 13, .  | 5.8 | 11        |
| 456 | Thermal stability of Al2O3-5 vol% SiC nanocomposite. Journal of Materials Science, 1995, 30, 321-333.  | 1.7 | 10        |
| 457 | Synthesis and dielectric characterisation of lead magnesium niobate from precipitation and freeze-drying methods. Journal of Materials Chemistry, 1998, 8, 2239-2244.  | 6.7 | 10        |
| 458 | A sol-gel derived 0.9Pb(Mg <sub>1/2</sub> Nb <sub>2/3</sub> )O <sub>3</sub> –0.1PbTiO <sub>3</sub><br>ceramic. Journal of Materials Research, 1999, 14, 537-545.   | 1.2 | 10        |
| 459 | Evidence of lower valence state of vanadium on the dielectric relaxation of ferroelectric<br>SrBi2(V0.1Nb0.9)2O9. Journal Physics D: Applied Physics, 2002, 35, 2254-2259.   | 1.3 | 10        |
| 460 | Nanosized Zincâ€Oxide Particles Derived from Mechanical Activation of<br>Zn <sub>5</sub> (NO <sub>3</sub> ) <sub>2</sub> (OH) <sub>8</sub> ·2H <sub>2</sub> O in Sodium<br>Chloride. Journal of the American Ceramic Society, 2002, 85, 273-275. | 1.9 | 10        |
| 461 | Ferroelectric properties of heterolayered lead zirconate titanate thin films. Journal of Electroceramics, 2006, 16, 425-430.   | 0.8 | 10        |
| 462 | Effect of <scp>(Bi,Gd)FeO<sub>3</sub></scp> Layer Thickness on the Microstructure and Electrical<br>Properties of <scp>BiFeO<sub>3</sub></scp> Thin Films. Journal of the American Ceramic Society, 2011,<br>94, 4291-4298.                      | 1.9 | 10        |
| 463 | Sonochemical synthesis and liquid crystal assembly of PS-b-PEO–titania aggregates. Chemical<br>Communications, 2012, 48, 8538.   | 2.2 | 10        |
| 464 | Charge defects-induced electrical properties in bismuth ferrite bilayered thin films. Materials<br>Research Bulletin, 2013, 48, 2973-2977.   | 2.7 | 10        |
| 465 | Encapsulating Oxygenâ€Ðeficient TiNb <sub>24</sub> O <sub>62</sub> Microspheres by Nâ€Đoped Carbon<br>Nanolayer Boosts Capacity and Stability of Lithiumâ€ŀon Battery. Batteries and Supercaps, 2020, 3,<br>1360-1369.                           | 2.4 | 10        |
| 466 | Hierarchically porous interlayer for highly permeable and fouling-resistant ceramic membranes in water treatment. Separation and Purification Technology, 2022, 293, 121092.   | 3.9 | 10        |
| 467 | Modification of indentation cracks in TZP ceramics by thermal treatment. Journal of Materials Science<br>Letters, 1988, 7, 560-562.  | 0.5 | 9         |
| 468 | The effects of hydroxide gel drying on the characteristics of co-precipitated zirconia-hafnia powders.<br>Journal of Materials Science, 1993, 28, 553-560.   | 1.7 | 9         |

| #   | Article   | IF  | CITATIONS |
|-----|---|-----|-----------|
| 469 | Crystallization in nanosized sol-derived zirconia precursors. Journal of Materials Science Letters, 1996, 15, 1680-1683.  | 0.5 | 9         |
| 470 | Ferroelectric lead scandium tantalate from mechanical activation of mixed oxides. Materials<br>Chemistry and Physics, 2002, 75, 157-160.  | 2.0 | 9         |
| 471 | TRANSPARENT TIO2-PMMA NANOHYBRIDS OF HIGH NANOCRYSTALLINITY AND ENHANCED NONLINEAR OPTICAL PROPERTIES. Journal of Nonlinear Optical Physics and Materials, 2005, 14, 281-297.   | 1.1 | 9         |
| 472 | Heterolayered PZT thin films of different thicknesses and stacking sequence. Journal of Materials Science, 2009, 44, 5375-5382.   | 1.7 | 9         |
| 473 | Microstructure and texture development in single layered and heterolayered PZT thin films. Journal of Materials Science, 2010, 45, 6187-6199.   | 1.7 | 9         |
| 474 | Multiferroic Behavior of Sn-Modified BiFeO[sub 3] Thin Films. Electrochemical and Solid-State Letters, 2010, 13, G83.   | 2.2 | 9         |
| 475 | Effect of bilayer structure and a SrRuO3 buffer layer on ferroelectric properties of BiFeO3 thin films.<br>Applied Physics A: Materials Science and Processing, 2012, 109, 57-61.   | 1.1 | 9         |
| 476 | PEO surface-decorated silica nanocapsules and their application in in vivo imaging of zebrafish. RSC<br>Advances, 2012, 2, 12392.   | 1.7 | 9         |
| 477 | Tunneling electroresistance effect in ultrathin BiFeO3-based ferroelectric tunneling junctions.<br>Applied Physics Letters, 2016, 109, .  | 1.5 | 9         |
| 478 | Alumina double-layered ultrafiltration membranes with enhanced water flux. Colloids and Surfaces<br>A: Physicochemical and Engineering Aspects, 2020, 587, 124324.  | 2.3 | 9         |
| 479 | MnO2 as an effective sintering aid for difficult-to-sinter LiTaO3-based ceramics: Densification and dielectric properties. Journal of Alloys and Compounds, 2020, 829, 154546.  | 2.8 | 9         |
| 480 | "Porous and Yet Dense―Electrodes for Highâ€Volumetricâ€Performance Electrochemical Capacitors:<br>Principles, Advances, and Challenges. Advanced Science, 2022, 9, e2103953.  | 5.6 | 9         |
| 481 | The microstructure of pressureless sintered silver-toughened alumina: an in situ TEM study. Materials<br>Science & Engineering A: Structural Materials: Properties, Microstructure and Processing, 1993,<br>161, 119-126. | 2.6 | 8         |
| 482 | The grain boundary modification of ceria-stabilized tetragonal zirconia polycrystals by a small amount of alumina addition. Journal of Materials Science Letters, 1993, 12, 702-705.                                      | 0.5 | 8         |
| 483 | Crystallization in seeded zirconia precipitates. Materials Letters, 1996, 27, 239-246.  | 1.3 | 8         |
| 484 | Synthesizing 0.9PZN–0.1BT by mechanically activating mixed oxides. Solid State Ionics, 1999, 120, 183-188.  | 1.3 | 8         |
| 485 | Cluster glass structure in nanohybrids of nonstoichiometric zinc ferrite in silica matrix. Applied<br>Physics Letters, 2001, 79, 3167-3169.   | 1.5 | 8         |
| 486 | Pb(Fe2/3W1/3)O3 by mechanical activation of coprecipitated Pb3Fe2O6 and WO3. Journal of Alloys and Compounds, 2002, 343, 156-163.   | 2.8 | 8         |

| #   | Article  | IF  | CITATIONS |
|-----|--|-----|-----------|
| 487 | Ferroelectric Pb(Mg1/3Nb2/3)O3 thin films by PLD at varying oxygen pressures. Microelectronic Engineering, 2003, 66, 926-932.  | 1.1 | 8         |
| 488 | Polarization behaviors of (Bi3.15Nd0.85)Ti3O12 thin films deposited by radio-frequency magnetron sputtering. Journal of Applied Physics, 2005, 98, 104106.   | 1.1 | 8         |
| 489 | Effect of Zn Concentration on Multiferroic and Fatigue Behavior of Bi[sub 0.90]La[sub 0.10]Fe[sub<br>1â^x]Zn[sub x]O[sub 3] Thin Films. Electrochemical and Solid-State Letters, 2010, 13, G105.               | 2.2 | 8         |
| 490 | Unit-cell determination of epitaxial thin films based on reciprocal-space vectors by high-resolution<br>X-ray diffractometry. Journal of Applied Crystallography, 2014, 47, 402-413.                           | 1.9 | 8         |
| 491 | Ferroelectric polarization relaxation in Au/Cu2O/ZnO/BiFeO3/Pt heterostructure. Applied Physics<br>Letters, 2015, 106, .   | 1.5 | 8         |
| 492 | Recent progress, developing strategies, theoretical insights, and perspectives<br>towardsÂhigh-performance copper single atom electrocatalysts. Materials Today Energy, 2021, 21,<br>100761.                   | 2.5 | 8         |
| 493 | Stabilization of perovskite phase and dielectric properties of 0.95PZN–0.05BT derived from mechanical activation. Journal of Alloys and Compounds, 2000, 297, 92-98.   | 2.8 | 7         |
| 494 | Structure and electrical properties of (100)-oriented Pb(Zn1/3Nb2/3)O3–Pb(Mg1/3Nb2/3)O3–PbTiO3 thin films on La0.7Sr0.3MnO3 electrode by chemical solution deposition. Thin Solid Films, 2008, 516, 5057-5061. | 0.8 | 7         |
| 495 | Formation and Evolution of Body entered Orthorhombic Mesophase in TiO <sub>2</sub> Thin Films.<br>Journal of the American Ceramic Society, 2009, 92, 1317-1321.  | 1.9 | 7         |
| 496 | Evaporationâ€induced Alignment of Cylindrical Mesopores in TiO <sub>2</sub> Thin Films. Journal of the<br>American Ceramic Society, 2010, 93, 365-369.   | 1.9 | 7         |
| 497 | Multiferroic behavior of BiFeO3–RTiO3 (Mg, Sr, Ca, Ba, and Pb) thin films. Journal of Applied Physics, 2010, 108, 026101.  | 1.1 | 7         |
| 498 | Effect of oxygen content during sputtering on the electrical properties of bismuth ferrite thin films.<br>Physica Status Solidi - Rapid Research Letters, 2011, 5, 190-192.                                    | 1.2 | 7         |
| 499 | Membrane Fouling: Microscopic Insights into the Effects of Surface Chemistry and Roughness.<br>Advanced Theory and Simulations, 0, , 2100395.  | 1.3 | 7         |
| 500 | Two-step pyrolysis of Mn MIL-100 MOF into MnO nanoclusters/carbon and the effect of N-doping.<br>Journal of Materials Chemistry A, 2022, 10, 8172-8177.  | 5.2 | 7         |
| 501 | The loading rate dependence of fracture strength in a reaction-sintered mullite ceramic. Journal of<br>Materials Science Letters, 1992, 11, 1201-1205.   | 0.5 | 6         |
| 502 | Effects of organic binders on the sintering of isostatically compacted zirconia powders. Journal of<br>Materials Science, 1992, 27, 63-67.   | 1.7 | 6         |
| 503 | Lead Zirconate Titanate Via Reaction Sintering of Hydroxide Precursors. Journal of Materials<br>Research, 1999, 14, 1503-1509.   | 1.2 | 6         |
| 504 | Seeding effect in the formation of Pb(Fe2/3W1/3)O3 via mechanical activation of mixed oxides. Solid State lonics, 2000, 132, 55-61.  | 1.3 | 6         |

| #   | Article  | IF         | CITATIONS |
|-----|--|------------|-----------|
| 505 | Strontium–titanate-doped lead metaniobate ferroelectric thin films. Applied Physics Letters, 2002, 81, 877-879.  | 1.5        | 6         |
| 506 | Ferroelectric and dielectric properties of 0.6SrBi2Nb2O9–0.4BiFeO3 thin films. Thin Solid Films, 2004, 460, 1-6.   | 0.8        | 6         |
| 507 | Ferroelectric Bi4–x Sm x Ti3 O12 Thin Films Fabricated by Pulsed Laser Deposition for Nv-RAM<br>Applications. Integrated Ferroelectrics, 2004, 61, 123-127.  | 0.3        | 6         |
| 508 | Enhancement of Magnetization and Curie Temperature in Sr2FeMoO6 by Ni Doping. Journal of the American Ceramic Society, 2006, 89, 672-674.  | 1.9        | 6         |
| 509 | Bilayered<br>BiFe <sub>0.95</sub> Mn <sub>0.05</sub> O <sub>3</sub> /Bi <sub>0.90</sub> La <sub>0.10</sub> FeO <sub>3Thin Films with Low Ferroelectric Coercivity and Large Remanent Polarization. Journal of the<br/>American Ceramic Society. 2010. 93. 2113-2116.</sub> | ubz<br>1.9 | 6         |
| 510 | Preparation and characterization of multiferroic CoFe2O4/Bi0.97Ce0.03FeO3 coaxial nanotubes.<br>Applied Physics A: Materials Science and Processing, 2012, 108, 829-834.   | 1.1        | 6         |
| 511 | Nanoscale phase mixture in uniaxial strained BiFeO3 (110) thin films. Journal of Applied Physics, 2015, 118, .   | 1.1        | 6         |
| 512 | Revealing the hydrothermal crystallization mechanism of ilmenite-type sodium niobate microplates:<br>the roles of potassium ions. CrystEngComm, 2017, 19, 5966-5972.   | 1.3        | 6         |
| 513 | Water Permeation through Conical Nanopores: Complex Interplay between Surface Roughness and Chemistry. Advanced Theory and Simulations, 2020, 3, 2000025.  | 1.3        | 6         |
| 514 | A quantitative X-ray diffraction phase analysis in the reaction-sintered mullite ceramics. Journal of<br>Materials Science Letters, 1992, 11, 1301-1304.   | 0.5        | 5         |
| 515 | Abnormal grain growth in alumina-doped hafnia ceramics. Journal of Materials Science, 1994, 29, 3577-3590.   | 1.7        | 5         |
| 516 | Sintering and microstructural development of La0.80Ca0.22CrO3. Journal of Materials Science<br>Letters, 1996, 15, 658-661.   | 0.5        | 5         |
| 517 | Title is missing!. Catalysis Letters, 2000, 64, 179-184.   | 1.4        | 5         |
| 518 | Doping effects of BiFeO3 in layered perovskite SrBi2Nb2O9. Materials Chemistry and Physics, 2002, 75, 105-109.   | 2.0        | 5         |
| 519 | Mechanical activation-induced B site order–disorder transition in perovskite<br>Pb(Mg1/3Nb2/3)O3–Pb(Mg1/2W1/2)O3. Materials Chemistry and Physics, 2002, 75, 211-215.  | 2.0        | 5         |
| 520 | Mechanically Activated Synthesis and Magnetoresistance of Nanocrystalline Double Perovskite<br>Sr2FeMoO6. Journal of the American Ceramic Society, 2005, 88, 2635-2638.  | 1.9        | 5         |
| 521 | Mesophase configurations and optical properties of mesoporous TiO2 thin films. Journal of Electroceramics, 2006, 16, 499-502.  | 0.8        | 5         |
| 522 | Ferroelectric and conductivity behavior of multilayered<br>PbZr0.52Ti0.48O3â^•Pb(Mg1â^•3Ta2â^•3)0.7Ti0.3O3â^•PbZr0.52Ti0.48O3 thin films. Journal of Applied Physics, 20<br>100, 034106.   | )(161.     | 5         |

JOHN WANG

| #   | Article  | IF   | CITATIONS       |
|-----|--|------|-----------------|
| 523 | Peculiar Dielectric Behaviors of (Na1/2Bi1/2)0.87Pb0.13TiO3Thin Films. Journal of the American Ceramic Society, 2007, 90, 111-115.   | 1.9  | 5               |
| 524 | Thickness-Dependent Magnetic Properties of Bismuth Ferrite Thin Films. Electrochemical and Solid-State Letters, 2011, 14, G57.   | 2.2  | 5               |
| 525 | Kinetic study of solid phase crystallisation of expanding thermal plasma deposited a-Si:H. Thin Solid<br>Films, 2012, 520, 5820-5825.  | 0.8  | 5               |
| 526 | Dielectric dispersion and impedance spectroscopy of B3+-doped Ba(Ti0.9Sn0.1)O3 ceramics. Ceramics<br>International, 2013, 39, S145-S148.   | 2.3  | 5               |
| 527 | Ferroelectricity and dipole-dipole interactions in NH4TiOF3 mesocrystals. Applied Physics Letters, 2013, 102, 232903.  | 1.5  | 5               |
| 528 | In situ electrochemical oxidation of electrodeposited Ni-based nanostructure promotes alkaline<br>hydrogen production. Nanotechnology, 2019, 30, 474001.   | 1.3  | 5               |
| 529 | Single Atom Electrocatalysis: Heterogeneous Single Atom Electrocatalysis, Where "Singles―Are<br>"Married―(Adv. Energy Mater. 9/2020). Advanced Energy Materials, 2020, 10, 2070037.  | 10.2 | 5               |
| 530 | Nanocrystalline 0.54PZN–0.36PMN–0.1PT of perovskite structure by mechanical activation. Materials<br>Science & Engineering A: Structural Materials: Properties, Microstructure and Processing, 2000,<br>286, 96-100.   | 2.6  | 4               |
| 531 | The B-site order-disorder transformation in<br>Pb(Sc <sub>1/2</sub> Ta <sub>1/2</sub> )O <sub>3</sub> triggered by mechanical activation. Journal of<br>Materials Science, 2004, 39, 5267-5270.  | 1.7  | 4               |
| 532 | Ferroelectric properties and leakage current mechanisms in SrBi2(V0.1Nb0.9)2O9 (SBVN) thin films.<br>Ceramics International, 2004, 30, 1505-1508.  | 2.3  | 4               |
| 533 | Ferroelectric crossovers triggered by isovalent A-site substitution in Pb0.7La0.2TiO3. Journal of Applied Physics, 2006, 100, 124101.  | 1.1  | 4               |
| 534 | Conducting perovskite LaNi0.6Co0.4O3 ceramics with glass additions. Journal of Electroceramics, 2006, 16, 313-319.   | 0.8  | 4               |
| 535 | Structure and Optical Properties of 0.1BiFeO3-0.9SrBi2Nb2O9 Thin Films Using a Modified Sol-Gel Technique. Journal of Sol-Gel Science and Technology, 2006, 37, 27-30.   | 1.1  | 4               |
| 536 | Pre-curing of supramolecular-templated mesoporous TiO2 films for dye-sensitized solar cells. Thin<br>Solid Films, 2010, 518, e34-e37.  | 0.8  | 4               |
| 537 | Compositionally graded bismuth ferrite thin films. Journal of Alloys and Compounds, 2011, 509, L319-L323.  | 2.8  | 4               |
| 538 | Thin film bilayers of multiferroic bismuth ferrite on Pt–Si substrate. Physica Status Solidi - Rapid<br>Research Letters, 2011, 5, 83-85.  | 1.2  | 4               |
| 539 | Leakage behaviors of ferroelectric (Bi3.15Nd0.85)Ti3O12 thin film derived from RF sputtering. Applied Physics A: Materials Science and Processing, 2011, 105, 997-1001.  | 1.1  | 4               |
| 540 | Multiferroic and fatigue behavior of<br>BiFe <sub>0.95</sub> Mn <sub>0.05</sub> O <sub>3</sub> /Bi <sub>0.90</sub> La <sub>0.10</sub> Fe <sub>0.85<br/>bilayered thin films. IEEE Transactions on Ultrasonics, Ferroelectrics, and Frequency Control, 2012,<br/>59, 14-20.</sub> | ōZn  | <syb>0.15</syb> |

| #   | Article   | IF  | CITATIONS |
|-----|---|-----|-----------|
| 541 | Origin of dielectric anomaly in double perovskite Ba2CoNbO6. Ceramics International, 2014, 40, 14607-14612.   | 2.3 | 4         |
| 542 | Exchange bias in tetragonal-like BiFeO 3 /Sr 2 FeMoO 6 bilayer. Journal of Magnetism and Magnetic<br>Materials, 2018, 464, 156-160.   | 1.0 | 4         |
| 543 | 3D spray-coated gradient profile ceramic membranes enables improved filtration performance in aerobic submerged membrane bioreactor. Water Research, 2022, 220, 118661.   | 5.3 | 4         |
| 544 | Mullitization in Al2O3-SiC nanocomposite: A case study of high temperature oxidation. Scripta<br>Materialia, 1996, 34, 935-940.   | 2.6 | 3         |
| 545 | A Monte Carlo simulation of B-site orderÂdisorder transformation in Pb(Sc1/2Ta1/2)O3triggered by mechanical activation. Journal of Physics Condensed Matter, 2002, 14, 8639-8653.                                     | 0.7 | 3         |
| 546 | Effects of precursor solution pH value and substrate texture on orientation degree of sol–gel-derived bismuth titanate thin films. Physica Status Solidi A, 2003, 198, 282-288.                                       | 1.7 | 3         |
| 547 | Ferroelectric Behaviors of W-Doped SrBi2Ta2O9 Thin Films. Integrated Ferroelectrics, 2004, 62, 163-169.   | 0.3 | 3         |
| 548 | Dielectric behaviors and phase separation in Pb(Ni1/2W1/2)O3–PbTiO3. Ceramics International, 2004, 30, 1361-1364.   | 2.3 | 3         |
| 549 | Phase Formation and Magnetoresistance of Double Perovskite Sr2FeMoO6. Journal of the American Ceramic Society, 2005, 88, 3279-3282.   | 1.9 | 3         |
| 550 | The low-temperature synthesis of BiFeO3–SrBi2Nb2O9 complexes by sol-gel process. Materials Letters,<br>2005, 59, 912-915.   | 1.3 | 3         |
| 551 | Effects of Ni doping on B-site ordering and magnetic behaviors of double perovskite Sr2FeMoO6.<br>Journal of Electroceramics, 2006, 16, 351-355.  | 0.8 | 3         |
| 552 | Ferroelectric properties of (Bi3.15 Nd 0.85 )Ti 3 O 12 with decreasing film thickness. Journal of Electroceramics, 2006, 16, 477-481.   | 0.8 | 3         |
| 553 | RF SPUTTERED BISMUTH FERRITE THIN FILMS: EFFECT OF ANNEALING DURATION. Functional Materials<br>Letters, 2008, 01, 221-224.  | 0.7 | 3         |
| 554 | Multiferroic, Optical, and Fatigue Behavior of BiFeO[sub 3] Thin Films with a Sintering Aid of CuO.<br>Electrochemical and Solid-State Letters, 2010, 13, G68.  | 2.2 | 3         |
| 555 | Freezeâ€dried graphene oxide modified with trimethylhexamethylene in the mix solvent for improved antiâ€corrosion property of epoxy. Journal of Applied Polymer Science, 2020, 137, 49139.                            | 1.3 | 3         |
| 556 | One-pot hydrothermal synthesis of fluorescent carbon quantum dots with tunable emission color<br>for application in electroluminescence detection of dopamine. Biosensors and Bioelectronics: X, 2022,<br>10, 100141. | 0.9 | 3         |
| 557 | Melded ceramic membranes: A novel fabrication method for ultrathin alumina membranes of high performance. Journal of the American Ceramic Society, 2022, 105, 6554-6569.  | 1.9 | 3         |
| 558 | An application of sol gelation in the dispersion mixing of ceramic-matrix composites. Journal of<br>Materials Science Letters, 1992, 11, 807-809.   | 0.5 | 2         |

| #   | Article   | IF  | CITATIONS |
|-----|---|-----|-----------|
| 559 | Unique Dielectric Behavior of<br>0.6Pb(Ni <sub>1/2</sub> W <sub>1/2</sub> )O <sub>3</sub> ·0.4PbTiO <sub>3</sub> Derived from<br>Mechanical Activation. Journal of the American Ceramic Society, 2003, 86, 791-794. | 1.9 | 2         |
| 560 | Structural and Optical Properties of Lead Titanate Nanowires Synthesized by Hydrothermal Method.<br>Key Engineering Materials, 2007, 336-338, 2157-2159.  | 0.4 | 2         |
| 561 | Microcrack coalescence in alumina-zirconia composites. Journal of Materials Science Letters, 1996, 15, 442-444.   | 0.5 | 2         |
| 562 | The closure of indentation cracks and strength recovery by low temperature ageing in Y-TZP. Scripta<br>Metallurgica Et Materialia, 1992, 27, 815-820.   | 1.0 | 1         |
| 563 | Crystallization of Lead Niobate Glass by Mechanical Activation. Journal of the American Ceramic Society, 2001, 84, 2691-2695.   | 1.9 | 1         |
| 564 | Nanocrystalline ferroelectric phases from mechanical activation of oxide compositions. Scripta<br>Materialia, 2001, 44, 1803-1806.  | 2.6 | 1         |
| 565 | Ferroelectric and Dielectric Properties of Pb(Mg1/3Ta2/3)0.7Ti0.3O3 Thin Films Derived from RF<br>Magnetron Sputtering. Journal of the American Ceramic Society, 2005, 88, 2769-2774.                               | 1.9 | 1         |
| 566 | Layer Structured Calcium Bismuth Titanate by Mechanical Activation. Journal of Metastable and Nanocrystalline Materials, 2005, 23, 47-50.   | 0.1 | 1         |
| 567 | Ferroelectric and Dielectric Properties of Bilayered PMN–PT/BNdT Thin Films. Journal of the American<br>Ceramic Society, 2006, 89, 2481-2485.   | 1.9 | 1         |
| 568 | Dielectric anomalies of Pb0.7La0.2TiO3-based perovskite. Journal of Electroceramics, 2006, 16, 277-282.   | 0.8 | 1         |
| 569 | Bilayered Pb(Zr,Ti)O3/(Bi,Nd)4Ti3O12 thin films. Journal of Electroceramics, 2006, 16, 459-462.   | 0.8 | 1         |
| 570 | Ferroelectric transitions by Ca substitution in Pb0.7Nd0.2TiO3. Journal of Applied Physics, 2008, 103, 084114.  | 1.1 | 1         |
| 571 | The Nanocrystallinity Enhancement of Sol-Gel Derived TiO <sub>2</sub> Nanoparticles by<br>Pre-Hydrothermal Treatment. Advanced Materials Research, 0, 415-417, 715-719.   | 0.3 | 1         |
| 572 | Mesoporous Hollow Carbon Derived from Soft-Templated Hydrothermal Process for Supercapacitor<br>Electrode. Key Engineering Materials, 0, 616, 134-140.  | 0.4 | 1         |
| 573 | Composites, Nanocomposites and Hybrid Materials. , 2016, , 21-36.   |     | 1         |
| 574 | Designing Energy Materials via Atomic-resolution Microscopy and Spectroscopy. Microscopy and Microanalysis, 2019, 25, 1998-1999.  | 0.2 | 1         |
| 575 | Large-Scale Epitaxial Growth of Ultralong Stripe BiFeO3 Films and Anisotropic Optical Properties. ACS<br>Applied Materials & Interfaces, 2022, , .  | 4.0 | 1         |
| 576 | The effects of a small Al2O3 addition on the crystallization and densification of Na2O-stabilized silica sols. Journal of Materials Science Letters, 1992, 11, 1029-1032.   | 0.5 | 0         |

JOHN WANG

| #   | Article  | IF  | CITATIONS |
|-----|--|-----|-----------|
| 577 | Post-Sinter Annealing of Pb0.7La0.2TiO3 Derived from Mechanical Activation. Integrated Ferroelectrics, 2004, 62, 35-41.  | 0.3 | 0         |
| 578 | Residual strains and dielectric properties of Pb/sub 0.7/La/sub 0.2/TiO/sub 3/-based perovskites. , 0, , .   |     | 0         |
| 579 | Dieletric anomalies in Pb0.7(1â^'x)Ca0.7xLa0.2TiO3. Applied Physics Letters, 2005, 87, 072904.   | 1.5 | 0         |
| 580 | Pb(Zn1/3Ta2/3)O3-PbTiO3 Derived from Mechanical Activation. Journal of the American Ceramic Society, 2006, 89, 060623005134009-???.  | 1.9 | 0         |
| 581 | Ferroelectric behaviors of sandwich structured PbZr0.52<br>Ti0.4803/Pb(Mg1/3Ta2/3)0.7Ti0.3O3/PbZr0.52Ti0.48O3 thin film. Journal of Electroceramics, 2006, 16,<br>453-457.   | 0.8 | 0         |
| 582 | Heterolayered Ferroelectric Pb(Zr,Ti)O <inf>3</inf> /(Bi,Nd) <inf>4</inf> Ti <inf>3</inf> O <inf>12</inf><br>Thin Films. Applications of Ferroelectrics, IEEE International Symposium on, 2007, , .                        | 0.0 | 0         |
| 583 | Phase transition behaviors of (Na1/2Bi1/2)1â^'x TiPb x O3 thin films. Journal of Electroceramics, 2008, 21, 336-339.   | 0.8 | 0         |
| 584 | Bilayered Pb(Zr,Ti)O3/(Bi,Nd)4Ti3O12 thin films. Journal of Electroceramics, 2008, 21, 331-335.  | 0.8 | 0         |
| 585 | Bismuth ferrite bilayered thin films of different constituent layer thicknesses. Journal of Alloys and Compounds, 2011, 509, 7742-7748.  | 2.8 | 0         |
| 586 | Effective control of polarity in Bi <sub>0.9</sub> La <sub>0.1</sub> FeO <sub>3</sub> thin films by<br>dopantâ€related internal bias. Physica Status Solidi (A) Applications and Materials Science, 2011, 208,<br>919-923. | 0.8 | 0         |
| 587 | Nanostructured Mesoporous Thick Films of Titania for Dye-Sensitized Solar Cells. Applied Mechanics and Materials, 0, 110-116, 540-546.   | 0.2 | 0         |
| 588 | Optical Properties of 0.95BiFeO <sub>3</sub> -RTiO <sub>3</sub> (R = Mg, Pb, Ba, Ca and Sr) Thin Films.<br>Integrated Ferroelectrics, 2012, 139, 1-6.  | 0.3 | 0         |
| 589 | Solar Energy and Energy Storage Materials and Devices Research in Singapore. , 2016, , 113-156.  |     | 0         |